Development/Plasticity/Repair

A Nedd4 E3 Ubiquitin Ligase Pathway Inhibits Robo1 Repulsion and Promotes Commissural Axon Guidance across the Midline

Madhavi Gorla, Karina Chaudhari, Maya Hale, Chloe Potter, and Greg J. Bashaw
Department of Neuroscience, Perelman School of Medicine, University of Pennsylvania, Philadelphia, Pennsylvania 19104

Commissural axons initially respond to attractive signals at the midline, but once they cross, they become sensitive to repulsive cues. In insects and mammals, negative regulation of the surface expression of Roundabout (Robo) receptors prevents premature response to Slit. We previously identified two mammalian Nedd4 interacting proteins, Ndfip1 and Ndfip2, that act analogously to *Drosophila* Commissureless (Comm) to recruit mammalian Robo1 to late endosomes. However, whether Nedd4 E3 ubiquitin ligases are required for Ndfip-mediated Robo1 regulation and midline axon crossing *in vivo* is not known. Here, we show using *in vitro* biochemical techniques and genetic analysis using embryonic mice of either sex that Nedd4-1 and Nedd4-2 are specifically required for Robo1 regulation and spinal commissural axon guidance. Biochemical data indicate that Robo1, Ndfip and Nedd4 form a ternary protein complex that depends on the presence of Ndfip, and these interactions are required for Robo1 endosomal sorting, ubiquitylation and degradation. Nedd4-1 and Nedd4-2 are expressed in commissural neurons in the developing spinal cord, and conditional deletion of Nedd4-1 or Nedd4-2 results in dose-dependent defects in midline crossing. We propose that Nedd4 E3 Ubiquitin ligases and their adaptor proteins Ndfip1 and Ndfip2 constitute a vital intracellular trafficking pathway required to downregulate Robo1 and promote midline crossing of commissural axons.

Key words: **axon guidance; midline; Nedd4 ubiquitin ligase; repulsion; slit-roundabout; spinal cord**

Significance Statement

During the development of the nervous system, many neurons extend their axons across the midline to establish circuits that are important for sensory, motor and cognitive functions. In order to cross the midline, axon responses to midline-derived cues must be precisely regulated. Here, we characterize an important intracellular trafficking pathway that regulates the membrane expression of the conserved Roundabout (Robo) axon guidance receptor- the receptor for the midline repellant Slit. We show that Nedd4 E3 Ubiquitin ligases and their Ndfip adapter proteins inhibit premature responses to Slit by promoting Robo degradation in precrossing commissural neurons in the developing spinal cord.

Introduction

During neuronal development, many neurons extend axons across the midline to establish circuits that are important for sensory, motor and cognitive functions (Dickson and Zou, 2010; Vallstedt and Kullander, 2013; Neuhaus-Follini and Bashaw, 2015b). In both insects and mammals, midline crossing is controlled by coordinating responses to attractive and repulsive signals secreted by the midline and other cells (Gorla and Bashaw, 2020). Commissural axons first respond to attractive signals, including members of the Netrin and Sonic Hedgehog families (Ishii et al., 1992; Mitchell et al., 1996; Serafini et al., 1996; Charron et al., 2003), which guide them to the midline. Once they have crossed, commissural axons become responsive to repellents, including Slit and Semaphorin proteins (Brose et al., 1999; Kidd et al., 1999; Zou et al., 2000). This change in response prevents commissural axons from re-entering the midline, allowing them to reach their contralateral synaptic targets.

Received Dec. 18, 2021; revised Aug. 9, 2022; accepted Aug. 11, 2022.

Author contributions: M.G., K.C., and G.J.B. designed research; M.G., K.C., M.H., C.P., and G.J.B. performed research; M.G., K.C., M.H., and C.P. analyzed data; M.G. and K.C. wrote the first draft of the paper; M.G., K.C., M.H., C.P., and G.J.B. edited the paper; M.G., K.C., M.H., and G.J.B. wrote the paper.

This work was supported by National Institutes of Health Grants R01 HD105946 and R35 NS097340 (to G.J.B.). We thank the members of the Bashaw Lab for discussions and comments on the manuscript; Hiroshi Kawabe and Nils Brose for the Nedd4-1 and Nedd4-2 conditional mutant mice; Thomas Mund and Hugh Pelham for the gift of Myc-Ndfip, PY-mutated Ndfip plasmids, and HA-tagged Nedd4 E3 ligase plasmids; Hideaki Fujita for the gift of FLAG-UB plasmid; and thank Wenqin Luo for allowing us to use her lab facilities.

M. Gorla's present address: Centre for Biotechnology, Institute for Science and Technology (IST), Jawaharlal Nehru Technological University Hyderabad, Kukatpally, Hyderabad 500 085, India.

The authors declare no competing financial interests.

Correspondence should be addressed to Greg J. Bashaw at gbashaw@pennmedicine.upenn.edu.

https://doi.org/10.1523/JNEUROSCI.2491-21.2022

Slit ligands and their Roundabout (Robo) receptors direct repulsive axon guidance at the midline (Blockus and Chédotal, 2016). Axons expressing Robo receptors are repelled from the midline in response to Slit. In both insects and mammals, commissural axons prevent premature responsiveness to Slit by regulating the expression and activity of Robo receptors (Keleman et al., 2002; Sabatier et al., 2004; Evans et al., 2015; Kinoshita-Kawada et al., 2019). In *Drosophila*, Commissureless (Comm) negatively regulates Robo1 surface expression to prevent repulsive signaling before midline crossing (Kidd et al., 1998; Keleman et al., 2002). Comm inhibition of Slit-Robo1 repulsion is essential for midline crossing. Before entering the midline, Comm expression is upregulated in commissural neurons, where it is thought to act by diverting newly synthesized Robo1 into the late endosomal compartment, thus preventing Robo1 expression at the cell surface (Keleman et al., 2002, 2005).

In contrast to Slit ligands and Robo receptors, *comm* does not appear to be conserved outside of insects (Keleman et al., 2002; Evans and Bashaw, 2012), raising the question of how Robo1 surface levels are negatively regulated in the mammalian spinal cord. Recently, we reported that Nedd4-family interacting proteins, Ndfip1 and Ndfip2 regulate mammalian Robo1 surface expression through an analogous mechanism, and promote the midline crossing of commissural axons in the developing spinal cord (Gorla et al., 2019). Like Comm, Ndfip1 and Ndfip2 can prevent the surface expression of mammalian Robo1 receptors by recruiting them to late endosomes. In addition, Ndfip proteins promote the ubiquitylation and degradation of Robo1, and point mutations that disrupt the interaction of Ndfip proteins with Nedd4 E3 ligases result in a failure to regulate Robo1 (Gorla et al., 2019). These findings raise the intriguing possibility that Ndfip proteins recruit one or more HECT-family E3 ligases to regulate Robo1 expression and commissural axon guidance in the spinal cord; however, a clear role for Nedd4 ubiquitin ligases in midline guidance has not been demonstrated.

Here, we investigate the role for Nedd4 family E3 ubiquitin ligases in commissural axon guidance in the developing mammalian spinal cord. Biochemical evidence shows that the Ndfip adapter proteins can interact with the seven vertebrate E3 ligases that we have tested, and these interactions require the WW-domain binding sites present in Ndfip proteins. Despite the promiscuity of these interactions, our biochemical data indicate that only Nedd4-1, Nedd4-2, and WWP-1 can promote the ubiquitylation and degradation of Robo1 *in vitro*. In addition, we present evidence that Nedd4-1 and Nedd4-2 can form a ternary complex with Ndfip proteins and Robo1 that depends on the presence of Ndfip proteins. We detect Nedd4-1 and Nedd4-2 transcript and protein in the developing spinal cord, including in commissural neurons at E11.5 when commissural axons cross the midline. Conditional knock-out of Nedd4-1, Nedd4-2, or both leads to defects in commissural axon guidance, where axons frequently fail to cross the floor plate. Together, our findings support a model in which the E3 ubiquitin ligase-mediated degradation of Robo1 receptors represents an important mechanism to prevent premature responsiveness to the midline repellant Slit.

Materials and Methods

Further information and requests for resources and reagents should be directed to the corresponding author.

Mouse strains and genotyping

Mice were maintained in a barrier facility at the Clinical Research Building, University of Pennsylvania. All mouse work was approved by the Institutional Animal Care and Use Committee at the University of Pennsylvania. Embryos were derived from timed breeding with *Nedd4-1f/+; Nedd4-2f/+; Wnt1-cre* male and *Nedd4-1f/f; Nedd4-2flf* or *Nedd4-1f/+; Nedd4-2fl+* female mice. The day of vaginal plug was counted as embryonic day (E)0.5, and embryos of either sex were harvested at E11.5 and E12.5. Genotypes were identified by PCR reactions using genomic DNA extracted from embryonic tails. For the Western blot analysis, E12.5 brain extracts were prepared from *Nedd4-1f/+; Nedd4-2f/+* (control), *Nedd4-1f/f;Wnt1-cre* (Nedd4-1cko), *Nedd4-2f/f; Wnt1-cre* (Nedd4-2cko), and *Nedd4-1f/f;Nedd4-2flf;Wnt1-cre* (Nedd4-1; Nedd4-2dcko) embryos.

Cell culture and transfection

COS-7 and 293T cells were maintained in DMEM, supplemented with 10% (v/v) fetal bovine serum (FBS) and a mixture of 1% penicillin and streptomycin at 37°C in a humidified 5% CO_2 incubator. Cultured cells were transiently transfected with Effectene transfection reagent (QIAGEN). All the transfections were conducted according to the manufacturer's instructions. E12.5 dissociated primary commissural neurons were isolated from E12.5 dorsal spinal cords and plated on acid-washed, Poly-D-Lysine (Sigma #P6407) and 2 mg/ml N-Cadherin (R&D Systems #1388-NC)-coated coverslips. Neurons were then cultured in neurobasal media supplemented with 10% FBS (Invitrogen #10437-028) and 1% penicillin/streptomycin/glutamine (Invitrogen #10378-016) mix for ~24 h at 37°C in a humidified 5% CO_2 incubator.

Cell lysates and immunoprecipitation

Twenty-four hours after transient transfections, cells were washed in PBS and subsequently lysed in lysis buffer (1× TBS supplemented with 1% Triton X-100 and 1× Complete Protease Inhibitor) for 30 min with gentle rocking at 4°C. Soluble proteins were recovered by centrifugation at 15,000 × *g* for 15 min at 4°C. Lysates were incubated with 1–2 µg of antibody overnight with gentle rocking at 4°C. After incubation, 30 µl of 50% slurry of proteinA and proteinG agarose (Invitrogen) were added, and samples were incubated for an additional 2 h with gentle rocking at 4°C. The immunocomplexes were washed three times with wash buffer (1× TBS supplemented with 0.1% Triton X-100 and 1× Complete Protease Inhibitor) and boiled at 90°C for 10 min in 2× Laemmli SDS sample buffer and analyzed by Western blotting. Proteins were resolved by SDS-PAGE and transferred to nitrocellulose membrane (GE Healthcare). Membranes were blocked with 5% dry milk dissolved in 1× PBS supplemented with 0.1% Tween 20 for 30 min to 1 h at room temperature on an orbital shaker and incubated with primary antibodies overnight at 4°C. After three washes in PBS/0.1% Tween 20 for 10 min, membranes were incubated with the appropriate horseradish peroxidase (HRP)-conjugated secondary antibody at room temperature for 1 h. Signals were detected using ECL Prime (GE Healthcare) according to manufacturer's instructions. Antibodies used: for immunoprecipitation, rabbit anti-Myc (1:200, Millipore #2475732) and for Western blotting, mouse anti-FLAG (1:1000, Sigma, F1804-50UG), mouse anti-HA (1:1000, BioLegend #901502), mouse anti-myc (1:1000, 9E10, DSHB), mouse anti-β tubulin (1:1000, E7, DSHB), rabbit anti-integrinβ1 (1:1000, Cell Signaling Technology #4706S), goat anti-rabbit HRP (1:10,000, Jackson ImmunoResearch #111-035-003), and goat anti-mouse HRP (1:10,000, Jackson ImmunoResearch #115-035-146).

For preparation of E12.5 mouse brain lysates, whole brains were harvested from control, *Nedd4-1cko*, *Nedd4-2cko*, and *Nedd4-1;Nedd4-2dcko* embryos and homogenized in lysis buffer (1× TBS supplemented with 1% Triton X-100 and 1× Complete Protease Inhibitor) by using a dounce homogenizer. Homogenized samples were incubated with gentle rocking at 4°C for 1 h and centrifuged at 15,000 × *g* in an ice-cold centrifuge. Supernatants were collected after centrifugation and Western blotting was performed as described above. Antibodies used: rabbit anti-Nedd4-1 (1:1000, Thermo Fisher Scientific #PA5-26930), rabbit anti-Nedd4-2 (1:1000, Sigma-Aldrich #HPA024618), mouse anti-β tubulin (1:1000, E7, DSHB), goat anti-rabbit HRP (1:10,000, Jackson ImmunoResearch #111-035-003), and goat anti-mouse HRP (1:10;000, Jackson ImmunoResearch #115-035-146).

Immunohistochemistry

Embryos at indicated time points were harvested and fixed in 4% Paraformaldehyde in PBS for 2 h at 4°C, cryoprotected in 30% sucrose in PBS overnight and frozen in a cryomold containing NEG-50 Frozen Section Medium (Thermo Fisher Scientific #6502) on dry ice and stored at −80°C. Frozen embryos were thin sectioned to yield 20-µm transverse sections with a cryostat. Antibody staining was performed on cryostat sections after blocking in 5% normal goat serum (NGS) in PBS containing 0.1% Triton X-100 or with 2% horse serum in PBS containing 0.1% Triton X-100 (for all anti-goat antibodies) for 1 h at room temperature. Sections were then incubated with primary antibodies overnight at 4°C in a humidified chamber. After three 10-min washes in PBS, sections were incubated with species-specific secondary antibodies conjugated to fluorophores at room temperature for 2 h. Antibodies used: rabbit anti-Nedd4-1 (1:100, Thermo Fisher Scientific #PA5-26930), rabbit anti-Nedd4-2 (1:100, Sigma-Aldrich #HPA024618), goat anti-Robo3 (1:200, R&D Systems #AF3076), goat anti-Robo1 (1:200, R&D Systems #AF1749), Alexa488 goat anti-rabbit (Invitrogen, 1:500), Cy3 donkey anti-goat (1:400, Jackson ImmunoResearch), goat anti-DCC (1:400, R&D Systems #AF844), and Alexa488 donkey anti-goat (1:500, Thermo Fisher Scientific #A11055).

Immunofluorescence

Transiently transfected COS-7 cells were washed once with ice-cold PBS, fixed for 20 min in 4% paraformaldehyde at room temperature, permeabilized with PBT (1× PBS supplemented with 0.1% Triton X-100) for 10 min and, then blocked in PBT + 5% NGS for 30 min at room temperature. Cells were then incubated with primary antibodies diluted in PBT + 5% NGS overnight at 4°C. After three 10-min washes in PBT, secondary antibodies diluted in PBT + 5% NGS were added and incubated for 1 h at room temperature. After incubation, cells were washed three times in PBT for 10 min and coverslips were mounted in Aquamount. For surface labeling, cells were washed with ice-cold PBS and blocked in PBS + 5% NGS for 20 min at 4°C. Cells were then incubated in primary antibodies diluted in PBS + 5% NGS for 30 min at 4°C, then washed three times in ice-cold PBS. Cells were fixed for 20 min at 4°C in 4% paraformaldehyde in PBS, followed by three washes in PBS and stained with other primary antibodies diluted in PBT + 5% NGS overnight at 4°C. After three washes in PBS, cells were incubated with secondary antibodies diluted in PBT + 5% NGS for 30 min at room temperature. Antibodies used: rabbit anti-Myc (1:500, Sigma, C3956-2MG), mouse anti-HA (1:1000, BioLegend #901502), Cy3 goat anti-mouse (1:1000, Jackson ImmunoResearch #115-165-003), and Alexa488 goat anti-rabbit (Invitrogen, 1:500).

In situ hybridization

DIG-labeled riboprobes were synthesized using a DIG RNA labeling kit (Roche) and hybridized on 20-µm transverse sections. Template for Nedd4-1, Nedd4-2, and Wwp-1 probes were amplified from the respective mouse ORF clones. mRNA signal was detected using AP-conjugated anti-DIG antibody and the signal was visualized by using the BCIP/NBT detection method. Primers used to amplify cDNA were: Nedd4-1 (5′-GAGACAAGTGGAGCAAGCTTTT-3′ and 5′-TTATTCTGCGGGCTCTTACTTC-3′), Nedd4-2 (5′-TGCAGCTTGCAGAAGACG-3′ and 5′-TTCCCATGAAACACCGCT-3′), and Wwp1 (5′-GGTTGCTTTCAGGTAGGATGTC-3′ and 5′-GTAAGCCTGTTCAGATTCTGGG-3′).

Open-book spinal cord preparations and DiI dye injections

E12.5 spinal cord open-book preparations were isolated as previously described (Lyuksyutova et al., 2003). Isolated open-books were fixed in 4% PFA for 45–60 min in 4°C. After fixation, open-books were incubated in ice-cold PBS until ready to inject with DiI. A series of multiple injections were made in the dorsal spinal cord cell bodies with Fast DiI (5 mg/ml DiI in ethanol) using a very fine needle. To remove any leaked DiI, open-books were washed in ice cold PBS. DiI-injected open-book preparations were incubated in ice cold PBS in the dark at 4°C for 3 d to let the dye diffuse into the axons. DiI-diffused open-books were then mounted in PBS on concave microscope slides.

Primary growth cone collapse assays

E12.5 dissociated primary dorsal commissural neurons were cultured as previously described. After ~20 h, the medium was replaced with Neurobasal supplemented with 1× B-27 (Thermo #A3582801) and 100 µM Heclin (Sigma-Aldrich #SML1396) and incubated at 37°C for 1.5 h. In the last 30 min of that incubation, 2 µg/ml recombinant Slit (R&D Systems #5444-SL) was added. Coverslips were then stained for DCC using immunohistochemistry to visualize and score commissural neurons. Growth cone collapse is scored blind to condition. Each square slide is imaged as five separate fields, one in each corner, and one in the center. Either 10 or 15 neurons with clear cell bodies and growth cones having no obvious overlap with other neurons are scored in each field for a total of either 50 or 75 neurons/slide. Growth cones with terminal extensions that appear to be smaller than the diameter of the cell body without obvious lamellopodia were scored as collapsed. Growth cones with terminal extensions larger than the diameter of the cell body and clearly visible lamellopodia were scored as extended.

Quantification and statistical analysis

Embryos were scored blind to genotype. Data are presented as mean values ± SEM. For statistical analysis, comparisons were made between genotypes using the Student's *t* test and ANOVA. Differences were considered significant when $p < 0.05$. The spinal commissure thickness was quantified on 5–10 sections per embryo. Two to five embryos were analyzed and quantified for each genotype. The ratio of the commissural axon bundle size was normalized to sibling controls. In order to control for any variability in the size of embryo, the values of commissure thickness were normalized with length of spinal cord (distance between the floor plate and the roof plate). Collapse assays were scored blind to experimental condition. Two to four embryos were analyzed and quantified for each condition with 50 or 75 neurons quantified per embryo. For Western blottings, densitometry analysis was performed and quantified from three independent experiments and normalized with tubulin levels.

Data and software availability

Confocal stacks were collected using a spinning disk confocal system (PerkinElmer) built on a Nikon Ti-U inverted microscope and processed by ImageJ and Adobe Photoshop software. All statistics and graphs were generated using Microsoft Excel or GraphPad Prism9.

Results

Nedd4 family E3 ubiquitin ligases interact with Ndfip proteins

In mammals, the Nedd4 family of E3 ubiquitin ligases includes seven closely related proteins: Nedd4 (Nedd4-1), Nedd4L (Nedd4-2), Itch, WWP1, WWP2, Smurf1, and Smurf2, and two more divergent ligases: NEDL1 and NEDL2 (Fig. 1*A*). All of these proteins are characterized by a unique domain architecture consisting of a N-terminal C2 domain, followed by WW domains and a C-terminal HECT domain. Earlier studies suggest that WW domains in E3 ligases can interact with proline-rich PY motifs in Ndfip proteins with high affinity and that these interactions are important for E3 ligase activation and also for substrate ubiquitylation (Fig. 1*B*; Harvey et al., 2002; Shearwin-Whyatt et al., 2004; Mund and Pelham, 2009, 2010).

We first sought to determine which of the HECT-family ligases can interact with Ndfip1 and Ndfip2 (Fig. 1). We focused our analysis on the seven most closely related HECT-family ligases and tested for interactions *in vitro* in 293T cells (Fig. 1*A*). We co-expressed Myc-tagged Ndfip proteins and HA-tagged E3 ligases and immunoprecipitation was performed using an anti-Myc antibody. In these experiments, all the Nedd4 E3 ligases co-immunoprecipitated with Ndfip1 and Ndfip2, confirming that Ndfip proteins and Nedd4 E3 ligases can physically interact (Fig. 1*C*). Since the PY motifs of both Ndfip1 and Ndfip2 are

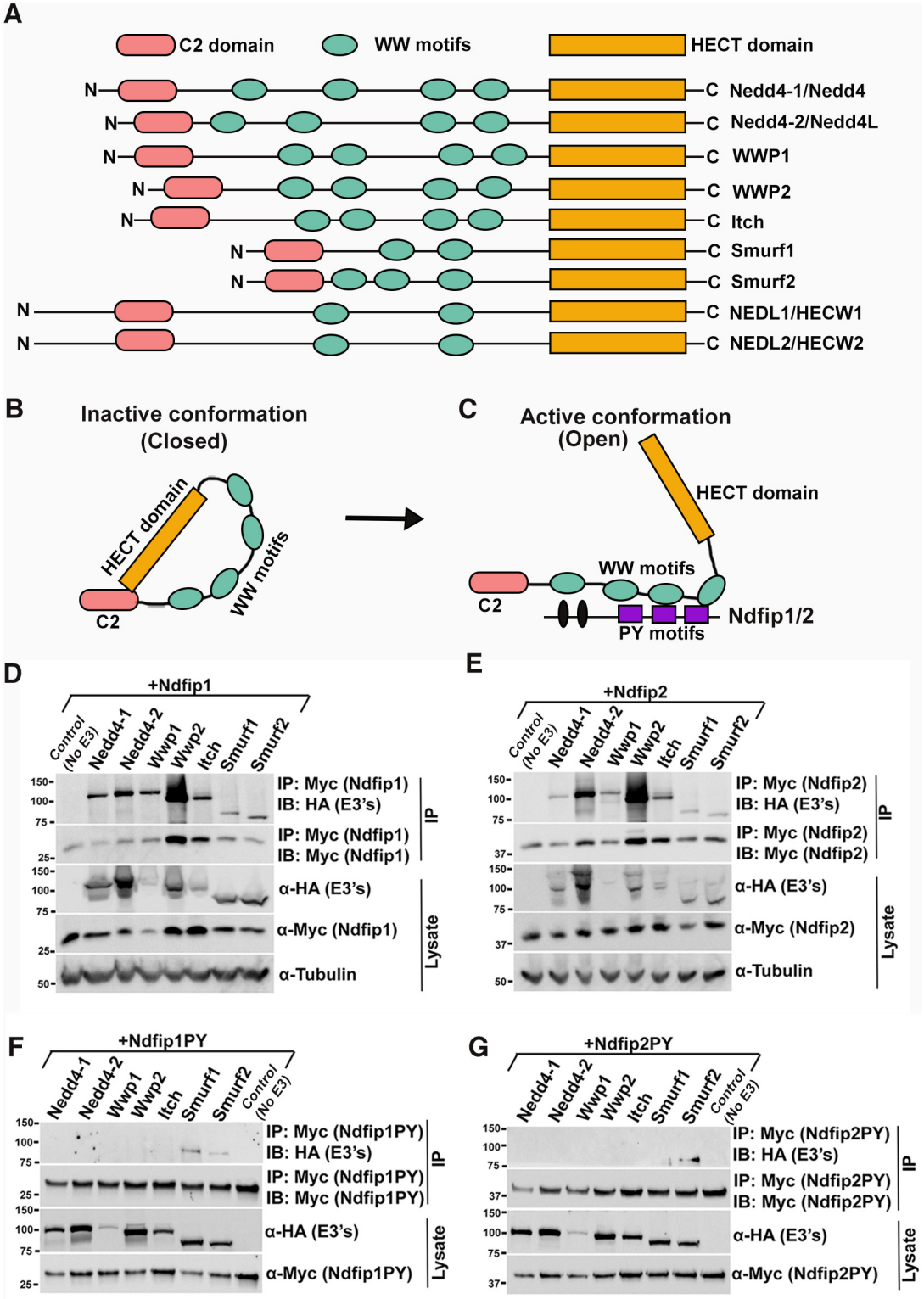

Figure 1. HECT domain containing Nedd4 family E3 ubiquitin ligases interact with the PY motifs of Ndfip proteins. ***A***, Schematic representation of the domain architecture of HECT domain containing Nedd4 family E3 ubiquitin ligases. All Nedd4 family E3 ligases are composed of three major domains: an amino-terminal C2 domain (pink), two to four WW domains (green), and a C-terminal HECT domain (yellow). These domains are responsible for lipid membrane binding, substrate/other protein interactions and catalytic activity, respectively. ***B***, ***C***, Schematic Illustration demonstrating how Nedd4 E3 ligase auto-inhibition is relieved on the interaction with their adaptor proteins, Ndfip1 and Ndfip2. ***D***, ***E***, HEK293T cells co-transfected with plasmids expressing HA-tagged Nedd4 family E3 ligases and with (***D***) Myc-Ndfip1 or Myc-Ndfip2 (***E***) Myc-Ndfip1^{PY} (***F***) or Myc-Ndfip2^{PY} (***G***) as indicated. Myc-tagged Ndfip proteins were immunoprecipitated with an anti-Myc antibody and co-immunoprecipitated HA-tagged E3 ligases were detected by Western blotting using an anti-HA antibody. The inputs (10% of total cell lysate used in the immunoprecipitation step) were analyzed using the indicated antibodies. All seven of the Nedd4 E3 ligases that we tested were detected in Ndfip1 or Ndfip2 immunoprecipitates in 293T cell lysates (***D***, ***E***). Immunoprecipitation of PY mutant variants of Ndfip1 (***F***) and Ndfip2 (***G***) fail to co-immunoprecipitate Nedd4 E3 ligases with the notable exception of Smurf1 and Smurf2 which can still interact with mutant Ndfip proteins. An anti-Tubulin antibody was used to control for equal protein loading. Molecular weights are indicated next to the Western blots.

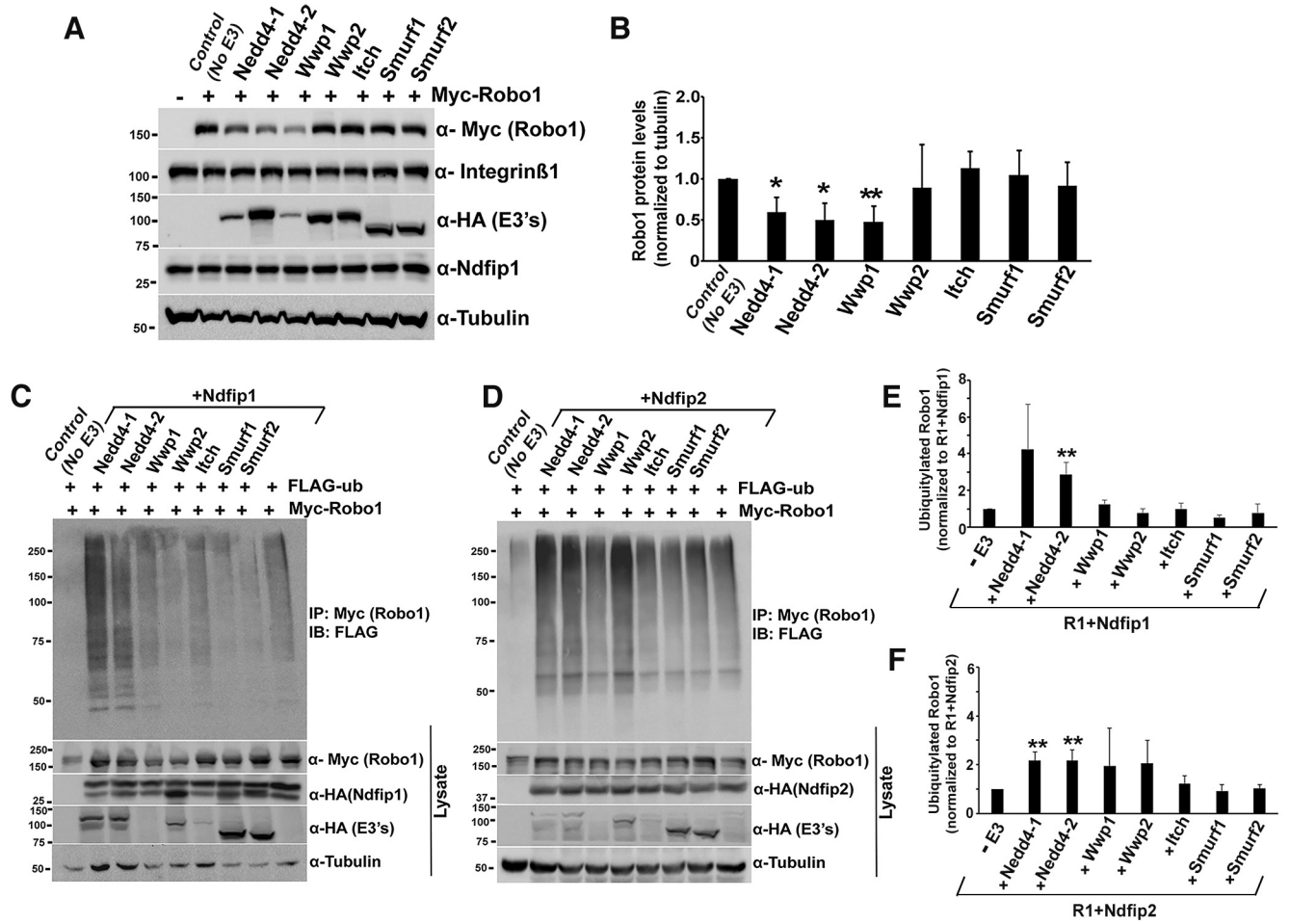

Figure 2. Nedd4-1/2 promote Robo1 ubiquitylation and degradation. ***A***, COS-7 cells were transiently co-transfected with Myc-tagged Robo1 and HA-tagged Nedd4 E3 ligases as indicated and the effect of E3 ligases on Robo1 protein levels was analyzed by Western blotting for Myc. ***B***, Quantitative representation of Robo1 protein levels that were normalized to tubulin levels. Nedd4-1, Nedd4-2, and WWP-1 lead to significant reduction in Robo1 protein levels, where the other E3 ligases do not. ***C***, ***D***, HEK293T cells were transiently co-transfected with Myc-Robo1, FLAG-Ub, HA-tagged E3 ligases, and HA-Ndfip1 or HA-Ndfip2 expression constructs as indicated. After 24 h of transfection, cell lysates were prepared and immunoprecipitated with an anti-Myc antibody and immunoprecipitates were Western blotted with an anti-FLAG antibody to detect the ubiquitylated Robo1. Ubiquitylated forms appear as smears. Ndfip1-mediated ubiquitylation of Robo1 was significantly enhanced by Nedd4-1 and Nedd4-2, whereas Nedd4-1, Nedd4-2, and Wwp2 enhance Ndfip2-mediated ubiquitylation of Robo1. Because co-expression of Ndfip proteins with WWP1 invariably leads to the degradation of WWP1, we were not able to reliably assess the effect of WWP1 on Robo1 ubiquitylation; however, given its strong effect on Robo1 degradation, it is likely that WWP1 can drive Robo1 ubiquitylation as well. ***E***, ***F***, Bar graphs denoting the amount of ubiquitylated Robo1 normalized to the amount of ubiquitylated Robo1 in the presence of Ndfip1 or Ndfip2. Error bars represent SEM. Significance was assessed by Student's *t* test $*p < 0.05$, $**p < 0.01$.

important for their interaction with WW domains (Harvey et al., 2002; Shearwin-Whyatt et al., 2004; Mund and Pelham, 2009, 2010), we also performed a similar set of immunoprecipitations with Ndfip proteins bearing mutations in their PY motifs. For the PY mutant variants of Ndfip, each PY motif was mutated from PxY to PAG to generate Ndfip1PY and Ndfip2PY. Most of the Nedd4 E3 ligases completely failed to co-immunoprecipitate with Ndfip1PY and Ndfip2PY, confirming the importance of PY motifs in Ndfip proteins for Nedd4 ligase interactions (Fig. 1*D*). Interestingly, these mutated Ndfip proteins can still bind to Smurf1 and Smurf2, albeit at a decreased level, suggesting that Ndfip proteins may have additional binding sites for Smurf proteins (Fig. 1*D*). Together, these data show that Ndfips can interact with all seven of the Nedd4 family ubiquitin ligases *in vitro* via their PY motifs.

Nedd4-1, Nedd4-2, and WWP1 can promote Robo1 degradation

The finding that all of the HECT-family ligases that we tested can associate with Ndfip proteins may reflect broad requirements for the Ndfip-mediated degradative pathway. However, given our interest in Robo1 regulation, we further tested whether these ligases can all contribute to the down regulation of Robo1 *in vitro* (Fig. 2). We co-expressed Myc-tagged Robo1, HA-tagged Ndfip proteins and Nedd4 family E3 ligases in 293T cells and quantified overall protein levels of Myc-tagged Robo1. Notably, among the seven ligases tested, only Nedd4-1, Nedd4-2, and WWP1 significantly reduced Robo1 protein levels, indicating that the association of E3 ligases with Ndfip proteins is not sufficient for their ability to regulate Robo1 levels (Fig. 2*A*,*B*). We next sought to determine whether the ability of E3 ligases to regulate Robo1 protein levels correlates with their ability to drive Robo1 ubiquitylation. To answer this question, we co-expressed Myc-tagged Robo1, FLAG- tagged Ubiquitin, HA-tagged Ndfip proteins and Nedd4 family E3 ligases in 293T cells. We performed immunoprecipitation studies with an anti-Myc antibody followed by Western blot analysis with anti-FLAG to monitor ubiquitylated Robo1 (Fig. 2*C*,*D*). We observe minimal Robo1 ubiquitylation under basal conditions. Consistent with our previously published observations (Gorla et al., 2019), expression of Ndfip1 and

Ndfip2 leads to a significant increase in the amount of ubiquitylated Robo1 compared with basal conditions. We see a further increase in Robo1 ubiquitylation in cells that co-expressed Nedd4-1 and Nedd4-2, but not in cells that express the other HECT family ligases, suggesting that Nedd4-1 and Nedd4-2 can specifically promote Robo1 ubiquitylation in the presence of Ndfip proteins (Fig. 2*C*,*D*). One caveat to these experiments is that we are unable to achieve consistent expression of WWP1 in these assays; indeed, WWP1 is always detected at significantly lower levels than the other ligases (Fig. 2*A*), suggesting that it is less stable under our experimental conditions. Given its robust effect on Robo expression levels (Fig. 2*A*,*B*), we believe it is highly likely that WWP1 can also target Robo1 for ubiquitylation.

Given Nedd4-1/2's ability to enhance Robo1 ubiquitylation and degradation, we next tested the importance of the ligase activity of Nedd4-1/2 in Ndfip-mediated Robo1 ubiquitylation. Nedd4 family E3 ligases are defined by a conserved C-terminal HECT domain, which requires an active site cysteine for ubiquitin transfer to substrate proteins. Using site-directed mutagenesis, we mutated these cysteine residues in Nedd4-1 and Nedd4-2 to generate catalytically inactive Nedd4-1C867A and Nedd4-2C942A. We hypothesized that catalytically inactive Nedd4-1/2 would not be able to promote Robo1 ubiquitylation. Indeed, while Robo1 is robustly ubiquitylated in 293T cells that co-expressed Ndfip1/2 and wild-type Nedd4-1/2, overexpression of either Nedd4-1C867A or Nedd4-2C942A fails to promote Ndfip-mediated Robo1 ubiquitylation. This suggests that Nedd4-1 and Nedd4-2 require their ligase activity to enhance Robo1 ubiquitylation in the presence of Ndfip proteins (Fig. 3*A*–*C*). As a second approach to test the importance of E3 ligase activity, we measured the level of Robo1 ubiquitylation in Ndfip1/2 and Nedd4-1/2 transfected 293T cells in the presence or absence of Heclin, which inhibits several HECT ligases in cultured cells (Fig. 3*D*,*E*; Mund et al., 2014). As before, the amount of Robo1 ubiquitylation is strongly increased in cells that co-express Ndfip1/2 along with either Nedd4-1 or Nedd4-2. However, Robo1 ubiquitylation is significantly decreased in cells that are treated with Heclin, indicating the importance of Nedd4 E3 ligase activity in Ndfip-mediated Robo1 degradation (Fig. 3*D*,*E*). Collectively, our data provide compelling evidence that a complex containing active Nedd4-1 or Nedd4-2 along with Ndfip proteins is important for the regulation of Robo1 turnover *in vitro*.

Nedd4, Ndfip, and Robo1 can form a protein complex *in vitro*

Since Nedd4-1 and Nedd4-2 specifically enhance Ndfip-mediated Robo1 ubiquitylation *in vitro*, we further explored the role of Nedd4-1 and Nedd4-2 in Robo1 regulation. Ndfip proteins interact with Nedd4 family E3 ubiquitin ligases to regulate the levels of specific substrate proteins (Foot et al., 2008; Mund and Pelham, 2009, 2010; Trimpert et al., 2017), and we have previously shown that Ndfip proteins can bind to Robo1 (Gorla et al., 2019). If Ndfip proteins can act as adaptor proteins between Robo1 and E3 ligases, we predicted that we could detect the presence of a Robo1/Ndfip/Nedd4 complex *in vitro*. To test this idea, we co-expressed Myc-tagged full-length Robo1 with HA-tagged Ndfip proteins along with HA-tagged Nedd4-1/2 in 293T cells and used an anti-Myc antibody to co-immunoprecipitate Robo1. Consistent with our previously published results (Gorla et al., 2019); both Ndfip1 and Ndfip2 readily co-immunoprecipitated with Robo1 (Fig. 4*A*,*B*). However, in the absence of Ndfip proteins, neither Nedd4-1 nor Nedd4-2 co-immunoprecipitate with Robo1, indicating that Robo1 and Nedd4 proteins are unlikely to directly interact (Fig. 4*A*,*B*). Consistent with this, while expression of Ndfip can relocalize Robo1 to intracellular puncta, expression of either Nedd4-1 or Nedd4-2 in the absence of co-expressed Ndfip proteins are unable to re-localize Robo1 to intracellular puncta (Fig. 5*A*). Furthermore, immunostaining for surface Robo1 in the presence or absence of Nedd4-1 or Nedd4-2 shows that neither Nedd4-1 nor Nedd4-2 can downregulate surface pools of Robo1 (Fig. 5*A*). In contrast to these observations, both Nedd4-1 and Nedd4-2 can be co-immunoprecipitated with Robo1 in the presence of Ndfip1 or Ndfip2 (Fig. 4*A*,*B*). This is consistent with a model in which Nedd4-1 and Nedd4-2 form a complex with Robo1 only in the presence of Ndfip proteins (Fig. 4*C*). Together with the ubiquitylation and degradation data (Figs. 2, 3), these protein interaction experiments support the model that Ndfip proteins bind to Robo1 and recruit Nedd4 ligases to drive its ubiquitylation and degradation (Fig. 4*C*).

These observations suggest that the formation of a ternary complex may be what confers the selectivity of Nedd4-1 and Nedd4-2 to drive Robo ubiquitylation and degradation. To further investigate this possibility, we tested whether Smurf-1 and Smurf-2, HECT family ligases that are unable to regulate Robo1, are also unable to form a protein complex with Robo1 and Ndfip. To our surprise, we were also able to detect a ternary complex between Ndfip proteins, Smurf and Robo1, indicating that other properties in addition to substrate recruitment are required for substrate specificity (Fig. 5*B*,*C*).

Nedd4-1 and Nedd4-2 are expressed in spinal commissural axons

Given the *in vitro* evidence that suggests a role for Nedd4-1/2 in Ndfip-mediated Robo1 degradation, we next sought to explore potential *in vivo* roles for the Nedd4-1 and Nedd4-2 during axon guidance. We first examined their expression during embryonic stages when spinal commissural axons are growing toward and crossing the floor plate. In E11.5 spinal cords, Nedd4-1 mRNA expression is specifically enriched in the floor plate region, motor column and in the dorsal root ganglia (DRG; Fig. 6*A*). Nedd4-2 mRNA expression also appears to be enriched in these regions, but to a lesser extent than Nedd4-1 (Fig. 6*B*). Both Nedd4-1 and Nedd4-2 mRNA signal is detected in the dorsal spinal cord in areas occupied by commissural neurons (Fig. 6*A*,*B*). No signal is detected using sense control probes, indicating that these mRNA expression patterns are specific (Fig. 6*A*,*B*). It is worth noting that Ndfip1/2 transcripts also have a comparable expression pattern to Nedd4-1/2 transcripts in the developing spinal cord (Gorla et al., 2019). In contrast to Nedd4-1 and Nedd4-2, we do not detect robust expression of WWP1 in the developing spinal cord (Fig. 6*C*); thus, we have restricted further analysis of expression and function to Nedd4-1 and Nedd4-2. Antibody staining reveals that both Nedd4-1 and Nedd4-2 are expressed in commissural axons at embryonic stage E11.5 (Fig. 6*D*,*E*). In addition, we also observed Nedd4-1/2 signal strongly in the DRG and moderately in motor neurons (Fig. 6*D*,*E*). Co-localization of Nedd4-1/2 with Robo3 indicates that Nedd4-1/2 are expressed in both the precrossing and postcrossing portions of commissural axons (Fig. 6*D*,*E*). Interestingly, in contrast to the Nedd4 proteins, Ndfip1 appears to be more strongly expressed in precrossing commissural axons relative to postcrossing axons (Gorla et al., 2019). This suggests both that lower expression of Ndfip proteins in postcrossing axons may prevent continued inhibition of Robo1 expression, and that Nedd4 may serve

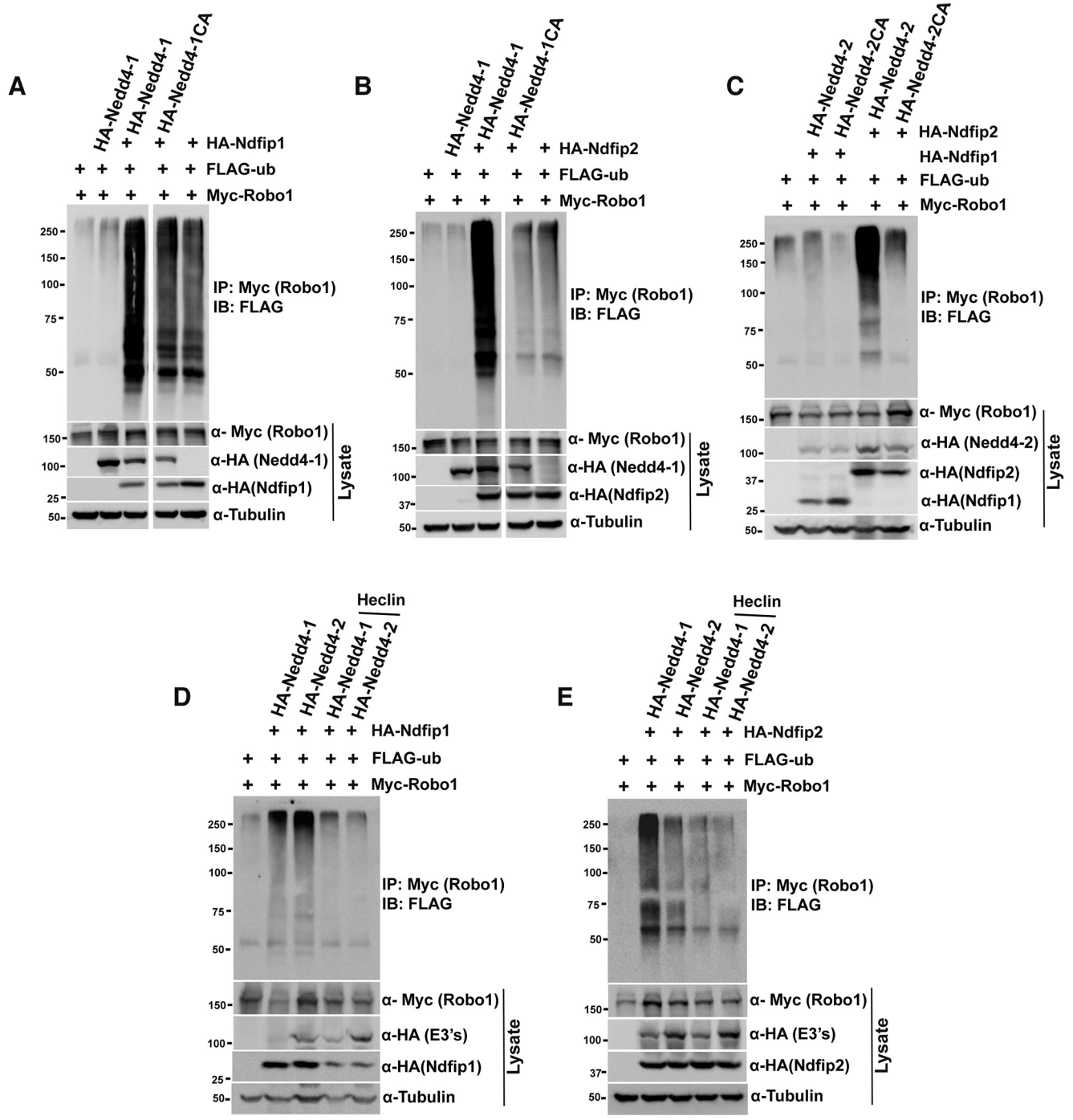

Figure 3. Nedd4-1 and Nedd4-2 ligase activity is required to promote Ndfip-mediated Robo1 ubiquitylation. ***A–E***, 293T cells transiently co-transfected with Myc-Robo1, FLAG-Ub, HA-tagged Nedd4-1 or Nedd4-1C867A or HA-tagged Nedd4-2 or Nedd4-2C942A and HA-Ndfip1 or HA-Ndfip2 expression constructs as indicated. After 24 h of transfection, cells were treated with 100 μM Heclin (***D***, ***E***) for 2 h. Cell lysates were immunoprecipitated with an anti-Myc antibody and immunoprecipitates were probed with an anti-FLAG antibody. Ndfip-mediated Robo1 ubiquitylation was significantly reduced on the co-expression of either catalytically inactive Nedd4-1C867A (***A***, ***B***) or Nedd4-2C942A (***C***) compared with wild-type Nedd4-1 or Nedd4-2. Upon treatment with Heclin, Ndfip/Nedd4mediated Robo1 ubiquitylation was considerably decreased (***D***, ***E***). The expression levels of Robo1 were analyzed with anti-Myc antibodies. The expression levels of Ndfip proteins and Nedd4 proteins were monitored with anti-HA antibodies. Ubiquitylated forms appear as smears. An anti-Tubulin antibody was used to control for equal protein loading.

additional functions unrelated to Robo1 regulation in post-crossing axons. To further characterize Nedd4-1 expression, we generated dissociated spinal commissural neurons from E11.5 mice. In these dissociated cultures, Nedd4-1 is expressed in Dcc-positive commissural neurons (Fig. 6*F*), further supporting the observations in transverse spinal cord sections. Notably, Nedd4-1/2 protein expression is decreased in the dorsal spinal cord in *Nedd4-1/2* conditional mutant spinal cord sections compared with control sections, confirming the specificity of Nedd4-1/2 antibodies (Fig. 7*A*,*B*).

Inhibition of Nedd4 E3 ligases leads to an increase in Slit response

Since Nedd4-1 and Nedd4-2 can promote Robo1 degradation *in vitro* and both are expressed in commissural axons *in vivo*, we next sought to evaluate whether the loss of Nedd4-1 and Nedd4-

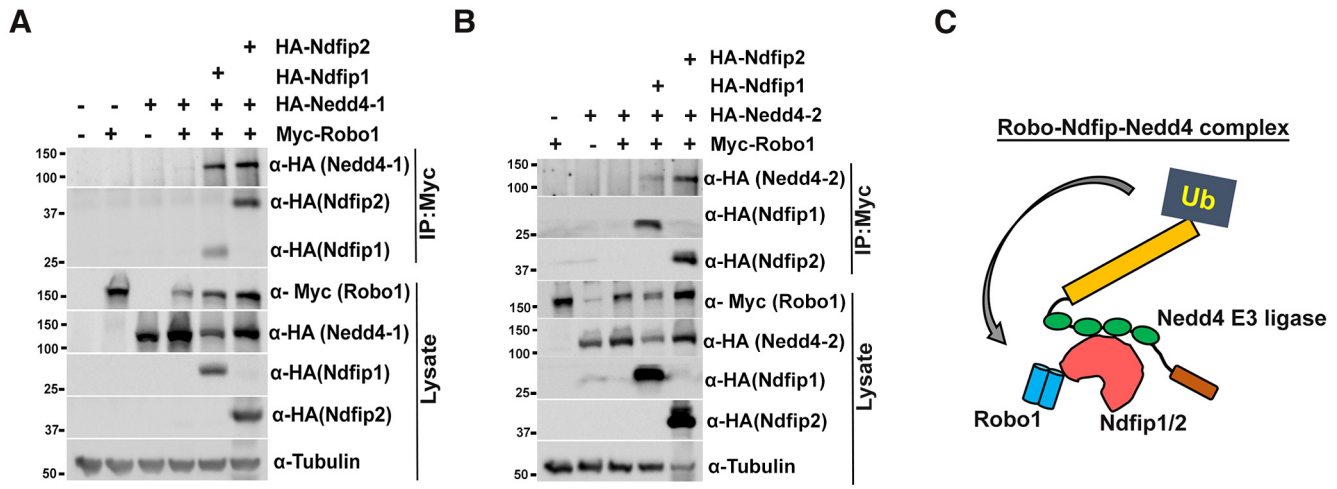

Figure 4. Nedd4-1/2 form a three-protein complex with Robo1 and Ndfip1/2 (***A***, ***B***) HEK293T cells were transiently co-transfected with Myc-Robo1, HA-tagged Nedd4-1 or HA-tagged Nedd4-2, and HA-Ndfip1 or HA-Ndfip2 expression constructs as indicated. After 24 h of transfection, cell lysates were prepared and immunoprecipitated with an anti-Myc antibody and immunoprecipitates were analyzed by Western blottings with an anti-HA antibody. Immunoprecipitation of Robo1 pulls down Nedd4-1 and Nedd4-2 only in the presence of Ndfip proteins. An anti-Tubulin antibody was used to control for equal protein loading. ***C***, Schematic illustration demonstrating the proposed mechanism of Ndfip1/2 and Nedd4 E3 ligase complex-mediated Robo1 ubiquitylation.

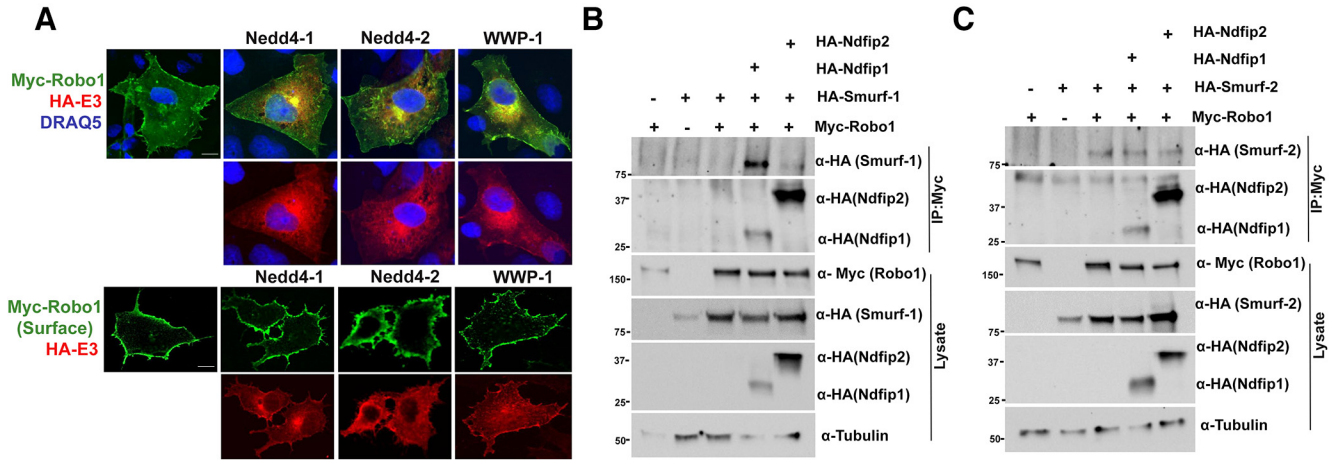

Figure 5. Nedd4 ligases are unable to downregulate surface pools of Robo1 in the absence of co-expressed Ndfip proteins. ***A***, Confocal micrographs of COS-7 cells expressing N-terminal Myc-Robo1 with C-terminal HA-Nedd4-1 or Nedd4-2-HA or Wwp1-HA. In cells that were transfected with either Myc-Robo1 alone or with Myc-Robo1 and HA-E3 ligases, Robo1 localization remains unchanged (top two rows). DRAQ-5 is a nuclear marker. Surface expression of Robo1 (green) was visualized by staining the N-terminal Myc-tag before fixation and permeabilization. The HA staining (red) reveals the expression of Nedd4-1 or Nedd4-2 or Wwp-1. Co-expression of Nedd4-1 or Nedd4-2 or Wwp-1 with Robo1 does not alter the surface pools of Robo1 (bottom two rows). ***B***, ***C***, HEK293T cells were transiently co-transfected with Myc-Robo1, HA-tagged Smurf-1 (***B***) and Smurf-2 (***C***) and HA-Ndfip1 or HA-Ndfip2 expression constructs as indicated. After 24 h of transfection, cell lysates were prepared and immunoprecipitated with an anti-Myc antibody and immunoprecipitates were Western blotted with an anti-HA antibody. Immunoprecipitation of Robo1 pulls down Smurf-1 (***B***) and Smurf-2 (***C***) in the presence of Ndfip proteins. An anti-Tubulin antibody was used to control for equal protein loading. Scale bars: 10 μm.

2 alters Robo1 levels and localization in commissural axons. Dorsal spinal cord-specific ablation of *Nedd4-1* and *Nedd4-2* was achieved by crossing Wnt1-cre transgenic mice with *Nedd4-1* or *Nedd4-2* floxed mice (Kawabe et al., 2010; Kimura et al., 2011). In wild-type E11.5 embryos, Robo1 is primarily localized to the postcrossing portion of commissural axons, with low levels detected on precrossing and crossing commissural axons (Fig. 8*A–E*). Our previously published results show that in *Ndfip1−/−; Ndfip2−/−* whole animal mutant embryos, Robo1 expression is significantly elevated in spinal commissural axons as they approach the midline, as well as in protein extracts from *Ndfip* mutant spinal cords (Gorla et al., 2019). Here, we analyzed Robo1 pixel intensity at the commissure in *Nedd4-1* and *Nedd4-2* conditional mutants. Unexpectedly, we did not observe a significant increase in Robo1 levels at the commissure in *Nedd4-1* and *Nedd4-2* single or double conditional mutants (Fig. 8). We were surprised to see no obvious effect on Robo1 expression levels and think this might reflect the use of conditional mutants, which only affects a subpopulation of commissural neurons, rather than whole animal knock-outs. Alternatively, the absence of detectable differences in Robo1 expression could either be because of incomplete Cre-dependent recombination of the Nedd4-1 and Nedd4-2 floxed alleles or potential redundancy among other HECT family ligases. Indeed, we still detect significant levels of Nedd4 proteins by both immunofluorescence and Western blotting in conditional knock-outs (Fig. 7).

As an alternative approach to evaluate whether disrupting Nedd4 ligase activity has an impact on Robo1 receptor expression and repulsive signaling, we made use of the Heclin small molecule inhibitor that we used successfully in our in vitro

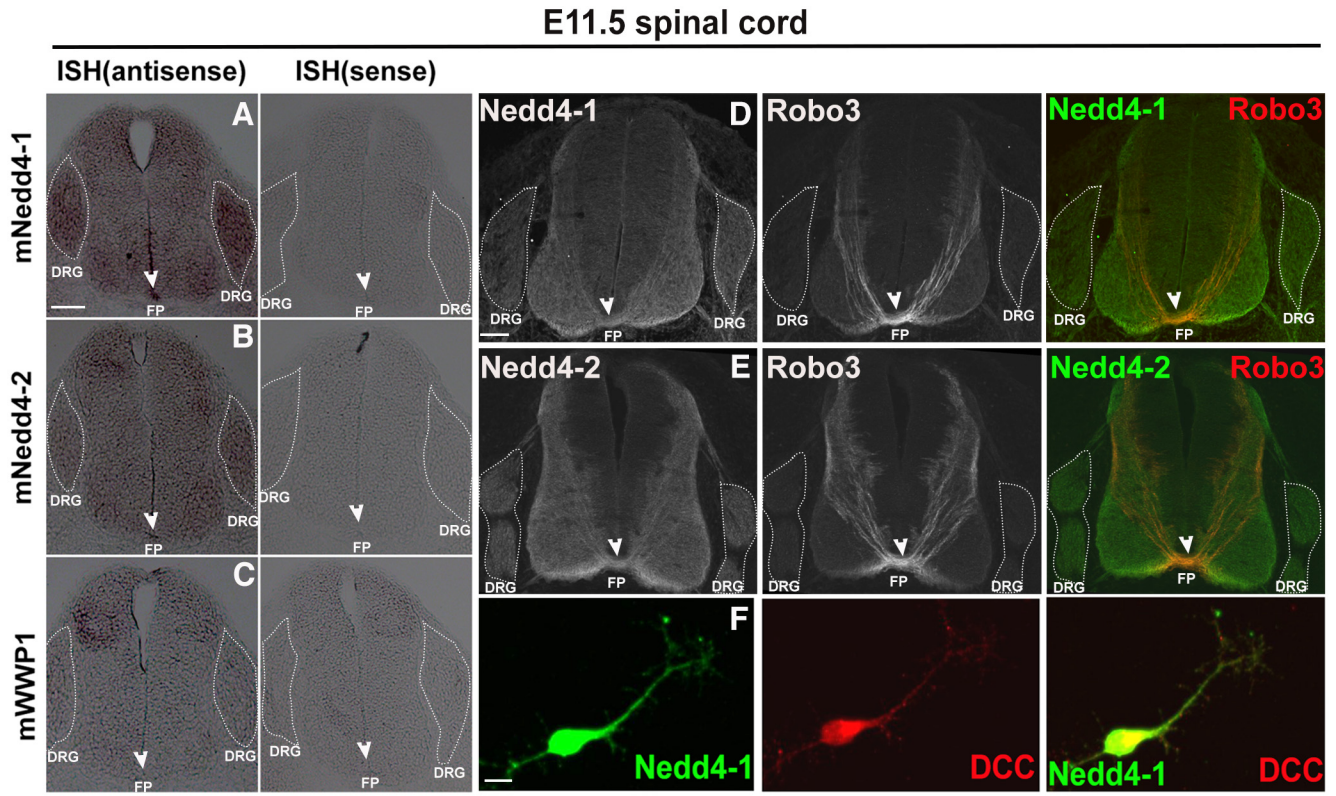

Figure 6. Nedd4-1 and Nedd4-2 are enriched in the developing spinal cord. ***A–C***, mRNA *in situ* hybridization reveals the expression of Nedd4-1 (***A***), Nedd4-2 (***B***), and Wwp1 (***C***) in E11.5 mouse spinal cords. mRNA probes to the sense strand serve as controls for the specificity of expression. ***D***, ***E***, Representative confocal images of transverse sections of a wild-type mouse E11.5 spinal cord labeled with anti-Nedd4-1 (***D***) or anti-Nedd4-2 (***E***) and anti-Robo3 antibodies. Co-localization of Nedd4-1 (***D***, in green) or Nedd4-2 (***E***, in green) with Robo3-positive commissural axons (***D***, ***E***, in red) demonstrates the presence of Nedd4 proteins in the commissural axon population. Both Nedd4-1 and Nedd4-2 are also strongly expressed in DRGs and moderately expressed in the motor column. ***F***, Double immunostaining of Nedd4-1 (green) and Dcc (red) in dissociated commissural neurons demonstrating the expression of Nedd4-1 in the cell body, axon and growth cone of commissural neurons. Scale bars: 100 μm (***A–E***) and 20 μm (***F***). FP and DRG denotes floor plate and dorsal root ganglion, respectively.

biochemical experiments to evaluate Robo1 ubiquitylation (Fig. 3*D*,*E*; Gorla et al., 2019). To assay effects of Heclin treatment on Robo1 repulsive function, we generated primary cultures of dissociated commissural neurons and measured growth cone collapse response to exogenously applied Slit protein. Consistent with our previously published results, treatment of E12.5 dissociated commissural neurons with recombinant Slit leads to a significant increase in growth cone collapse (Fig. 8*I*; Chaudhari et al., 2021). Wild-type cultures from E12.5 mice exhibit a baseline growth cone collapse of ~40% and treatment with Heclin has no significant effect on this baseline (Fig. 8*E–I*). In contrast, treatment of wild-type cultures with Slit, leads to a consistent and significant increase in growth cone collapse of ~60%. Strikingly, including Heclin in combination with Slit-treatment results in a significant increase in the Slit response and ~80% of growth cones exhibit collapsed morphology. Taken together with our biochemical data, these results strongly suggest that by inhibiting the activity of Nedd4 family E3 ligases, Robo surface expression and repulsive response to Slit are elevated.

Nedd4 conditional mutants have deficits in spinal commissural axon guidance

Despite the lack of discernible Robo1 expression differences observed by immunofluorescence, the observation that dissociated commissural neurons exhibit an increased collapse response to Slit when they are treated with Heclin suggests that Robo receptor activity is indeed elevated. Therefore, we reasoned that careful analysis of commissural axon guidance phenotypes might be more sensitive for observing changes indicative of premature midline repulsion. Thus, to examine the role of Nedd4-1 and Nedd4-2 in commissural axon guidance, we analyzed embryonic spinal commissural axons in *Nedd4-1* and *Nedd4-2* conditional knock-out mice. The *Nedd4-1* and *Nedd4-2* floxed mice were previously described (Kawabe et al., 2010; Hsia et al., 2014). Dorsal spinal cord-specific ablation of *Nedd4-1* and *Nedd4-2* was achieved by crossing *Nedd4-1* or *Nedd4-2* floxed mice with Wnt1-cre transgenic mice. Compared with Cre-negative sibling control embryos, Nedd4-1 or Nedd4-2 protein is reduced in the dorsal regions of *Nedd4-1* or *Nedd4-2* conditional mutant embryonic spinal cords (Fig. 7*A*,*B*). Furthermore, the levels of Nedd4-1 and Nedd4-2 protein in single and double mutant E12.5 brain lysates were significantly decreased in conditional mutants compared with control embryonic lysates (Fig. 7*C*). We next analyzed commissural axon guidance defects in *Nedd4-1f/f; Wnt1-cre* and *Nedd4-2f/f; Wnt1-cre* single mutant embryos by immunostaining transverse sections of the spinal cord with antibodies to the Robo3 receptor and measuring the thickness of the floor plate commissure. Robo3 is specifically expressed in all populations of dorsal commissural axons as they project toward and across the midline and is thus an ideal marker to monitor commissure formation. To exclude any variability in the size of embryo, the values of Robo3-positive commissure thickness were normalized with dorsal-ventral length (SC length) of the spinal cord. We observed a significant reduction in the thickness of the Robo3-positive commissure in *Nedd4-1* and *Nedd4-2* single mutant embryos at E11.5, indicating that fewer axons crossed the floor plate at the ventral midline in these mutants (Fig. 9*A*,*C*).

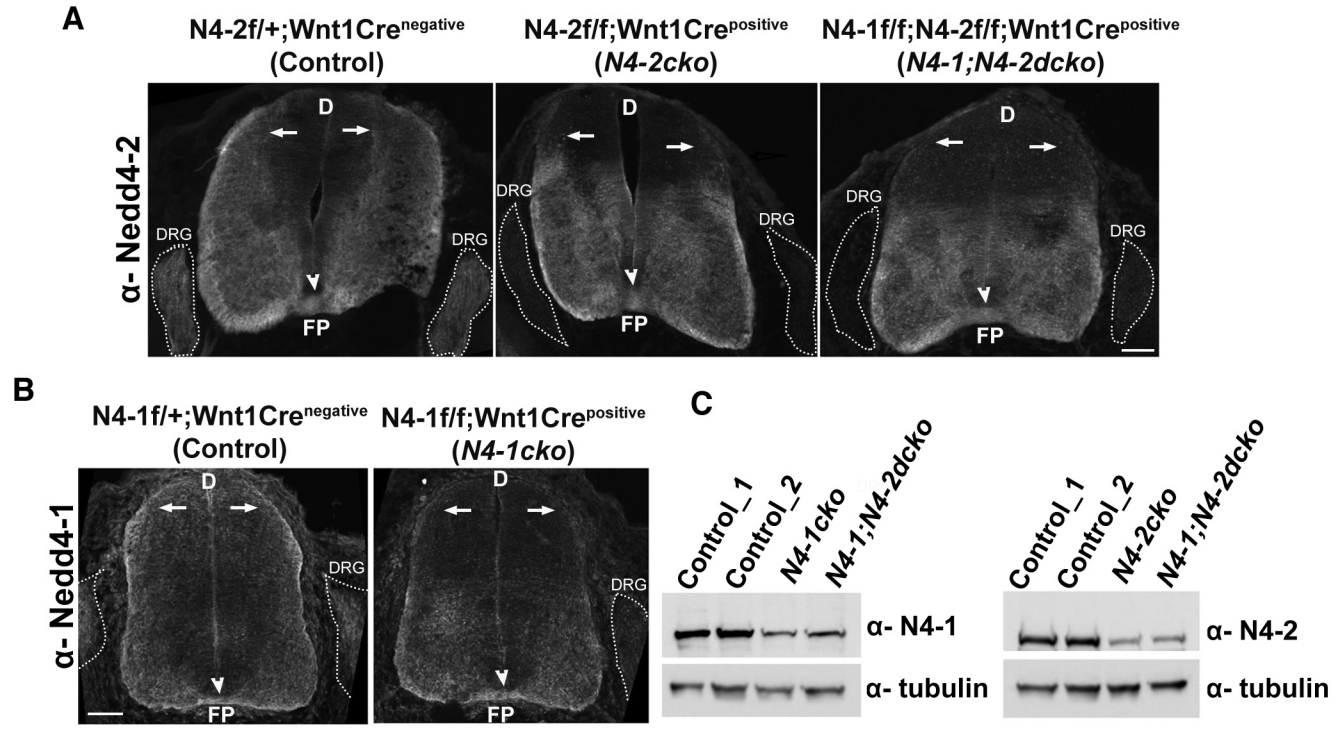

Figure 7. Nedd4-1 and Nedd4-2 expression is reduced in dorsal spinal cords of *Nedd4-1* and *Nedd4-2* conditional mutants, respectively. ***A***, Transverse sections of E11.5 Nedd4-2f/+;Wnt-cre^{negative} (Control) and Nedd4-2f/f;Wnt-cre^{positive} (*Nedd4-2cko*) or Nedd4-1f/f; Nedd4-2f/f;Wnt-cre^{positive} (*Nedd4-1;Nedd4-2dcko*) embryonic spinal cords immnunostained with an anti-Nedd4-2 antibody. ***B***, Transverse sections of E11.5 Nedd4-1f/+;Wnt-cre^{negative} (Control) and Nedd4-1f/f;Wnt-cre^{positive} (*Nedd4-1cko*) embryonic spinal cords immnunostained with an anti-Nedd4-1 antibody. In control spinal cord sections, both Nedd4-1 and Nedd4-2 were strongly expressed in commissural axons, in DRGs and moderately expressed in the motor column. Whereas in Wnt1Cre-depleted *Nedd4-1* or *Nedd4-2* spinal cords, Nedd4-1/2 protein expression was decreased in the dorsal spinal cord and in DRGs demonstrating the specificity of the Wnt1Cre-dependent depletion. ***C***, Brain extracts from E12.5 wild-type and *Nedd4-1cko* or *Nedd4-2cko* mutants were immunoblotted with anti-Nedd4-1 and anti-Nedd4-2 antibodies. Anti-Tubulin antibody was used as a loading control. Nedd4-1 and Nedd4-2 protein levels were decreased in *Nedd4* conditional mutant brain lysates compared with control brain lysates. Scale bars: 100 μm. FP and DRG denotes floor plate and dorsal root ganglion, respectively. D, dorsal.

Nedd4-1 and Nedd4-2 share similar expression patterns and are both capable of enhancing Robo1 ubiquitylation *in vitro* suggesting a compensatory mechanism that might explain why single mutants reveal only partial disruption in midline crossing. We thus sought to evaluate the consequence of simultaneous removal of both Nedd4-1 and Nedd4-2. We generated double mutants by crossing *Nedd4-1f/+;Nedd4-2f/+* mice with *Nedd4-1f/+;Nedd4-2f/+;Wnt1-cre* mice. If Nedd4-1 and Nedd4-2 work together to promote midline crossing, we would expect the double mutants to show significantly stronger disruptions in midline crossing than single mutants. Indeed, double mutant embryos have thinner Robo3-positive commissures than either *Nedd4* single mutant (Fig. 9*A*,*C*). We also analyzed commissural axon guidance in *Nedd4-1* and *Nedd4-2* conditional mutant spinal cords at the embryonic stage E12.5, where many more commissural axons have completed midline crossing. At this embryonic stage as well, we observed a significant decrease in Robo3-positive commissural thickness in *Nedd4-1f/f; Nedd4-2f/f;Wnt1-cre* double mutants (Fig. 9*B*,*D*). Taken together, our results strongly suggest that Nedd4-1 and Nedd4-2 work together to promote midline crossing of commissural axons. Moreover, it is worth noting that the decrease in commissure thickness observed in *Nedd4-1* and *Nedd4-2* conditional mutants is reminiscent of *Ndfip1* and *Ndfip2* whole animal knock-outs, consistent with the idea that Ndfip proteins and Nedd4 ligases likely act in concert to guide commissural axons in the embryonic spinal cord.

While our examination of ventral commissure thickness is consistent with a reduction in midline crossing, immunostaining of transverse spinal cord sections does not allow us to resolve the behavior of the precrossing and postcrossing subsets of commissural axons, since once axons reach the floor plate, they become intermingled with axons from the other side of the midline. For a more detailed analysis of the axon guidance defects in *Nedd4* mutants, we performed a series of unilateral dye-labeling experiments to document the behavior of small groups of axons as they approach and cross the midline (Fig. 10*A*). We dissected open-book spinal cord preparations from E12.5 *Nedd4-1f/f;Wnt1-cre* and *Nedd4-2f/f;Wnt1-cre* single mutant embryos and DiI was injected into one side of the dorsal spinal cord. Note that this is a stage when most commissural axons have crossed the midline. Indeed, in control embryos at E12.5, the majority of labeled axons cross the midline and turn anteriorly (Fig. 10*B*). In contrast, labeled axons in *Nedd4-1* and *Nedd4-2* single mutant spinal cords frequently stop within or just short of the floor plate and fail to make the correct anterior turn (Fig. 10*C*,*D*). Here, again, dye injections in *Nedd4-1*, *Nedd4-2* double conditional knockouts show even stronger guidance defects than the single mutants with many more axons stalling at the floor plate (Fig. 10*E*,*F*). Combined with the data showing a decrease in commissure thickness, these observations further support the model that Nedd4-1 and Nedd4-2 facilitate the guidance of spinal commissural axons across the midline.

Discussion

This study documents a role for Nedd4 ubiquitin ligases in commissural axon guidance. Ndfip adaptor proteins bind to E3 ubiquitin ligases to promote the ubiquitylation and degradation of

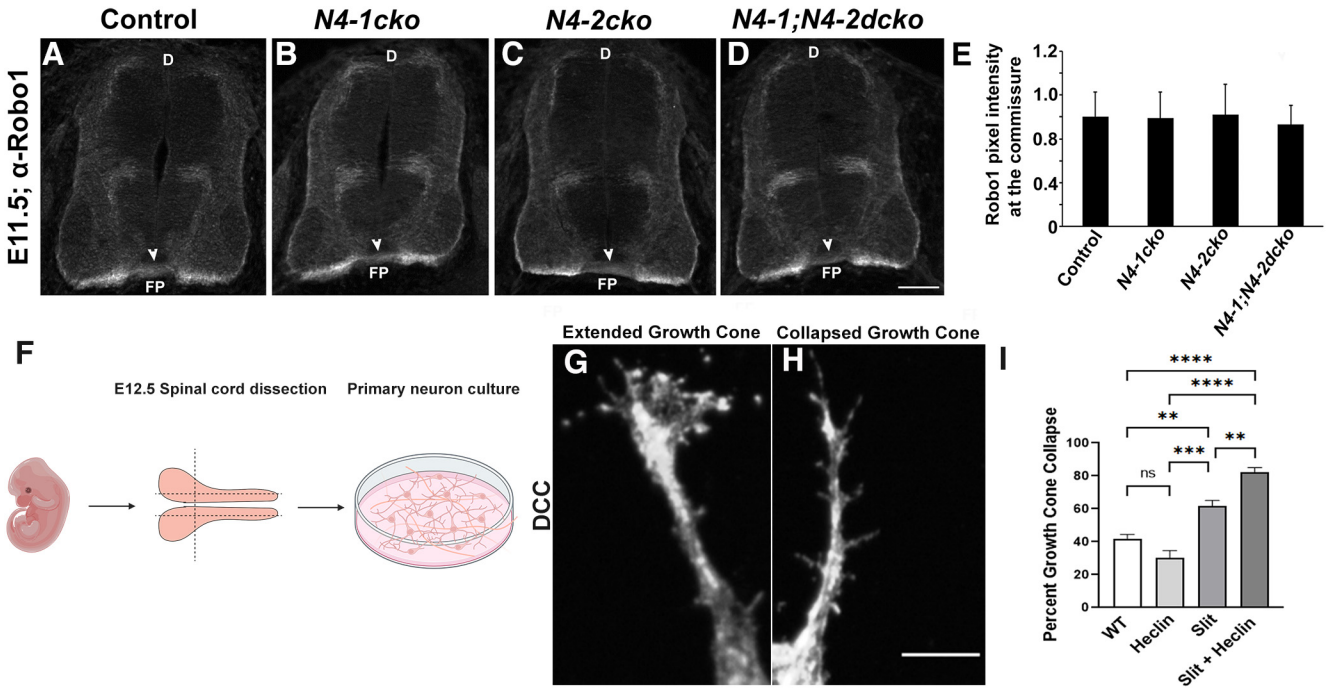

Figure 8. Inhibition of Nedd4 ligase activity with Heclin leads to increased Slit response. ***A–D***, Transverse sections of E11.5 control, *Nedd4-1cko*, *Nedd4-2cko*, or *Nedd4-1;Nedd4-2dcko* spinal cords immunostained with an anti-Robo1 antibody. ***E***, Quantitative representation of Robo1 pixel intensity at the commissure in control, *Nedd4-1cko*, *Nedd4-2cko*, or *Nedd4-1;Nedd4-2dcko* spinal cord sections. Robo1 levels at the ventral commissure appear to be unaffected in conditional Nedd4 mutants. Scale bars: 100 μm. FP denotes floor plate. D, dorsal. ***F***, Schematic of E12.5 spinal cord dissection. Horizontal dashed lines indicated cut locations to isolate the dorsal spinal cord for dissociated neuron culture. Dissociated commissural neurons showing representative images of extended and collapsed growth cones used in growth cone collapse scoring. Commissural neurons were identified with DCC immunostaining. ***G***, ***H***, Representative images of an extended (***G***) and collapsed growth cone (***H***). ***I***, Quantification shows percent of axons with collapsed growth cones. Wild-type (WT) neurons show increased collapse when treated with Slit (WT = 41.67 ± 2.688% and bath application of Slit = 61.56 ± 3.548%; $p = 0.0016$). Neurons treated with bath application of Heclin alone show no significant difference from WT (WT = 41.67 ± 2.688% and Heclin = 30 ± 4.67%; $p = 0.2683$). Bath application of both Slit and Heclin show increased Slit response when compared with Slit alone (Slit = 61.56 ± 3.548% and Slit + Heclin = 82 ± 3.00%; $p = 0.0012$). Data are presented as mean percentage ± SEM. Significance was assessed by one-way ANOVA with Tukey's multiple comparisons test. Number of trials: $n = 2$ for Heclin; $n = 6$ for WT, Slit and Slit + Heclin (50 or 75 neurons for each condition/trial). Scale bars: 10 μM.

Robo1. Although Ndfip proteins can interact with several E3 ubiquitin ligases, only a subset of these ligases promotes Robo1 degradation. Using HECT ligase inhibitors and catalytically inactive variants, we demonstrate the requirement for Nedd4-1/2 activity in Robo1 ubiquitylation. Further, we demonstrate that Nedd4 proteins form a ternary complex with Ndfip and Robo1 that depends on Ndfip. Finally, we show that Nedd4 proteins are expressed in commissural axons and conditional knock-outs of Nedd4-1 or Nedd4-2 show a significant reduction in midline crossing in the spinal cord. Simultaneous removal of Nedd4-1 and Nedd4-2 results in significantly stronger phenotypes suggesting that Nedd4-1 and Nedd4-2 act in parallel to regulate commissural axon guidance. Together, our results support a model in which Nedd4 degradation of Robo1 in precrossing commissural axons promotes midline crossing by preventing premature responsiveness to Slit.

Requirement of E3 ubiquitin ligases in the regulation of the Robo1 receptor

Previously we showed that Robo1 levels are significantly increased in *Ndfip* mutants (Gorla et al., 2019). The observation that Robo1 levels appear to be unaffected in *Nedd4-1/2* conditional mutants is surprising since our *in vitro* results suggest that the overexpression of Nedd4-1/2 can increase Ndfip-mediated Robo1 ubiquitylation and degradation. One potential explanation for this apparent discrepancy, could be that *Nedd4-1* and *Nedd4-2* are depleted only in the Wnt1-specified dI1 and dI2 subsets of commissural axons, whereas *Ndfip1*and *Ndfip2* were depleted in all commissural neuron populations in the spinal cord. Notably, while the decrease in commissural thickness in *Nedd4-1/2* conditional mutants is similar to *Ndfip1/2* knock-outs, the phenotype is stronger in *Ndfip1/2* mutants (~36% of commissural axons fail to cross) than in *Nedd4-1/2* conditional mutants (~25% of commissural axons fail to cross). Importantly, despite the apparent absence of increased Robo1 expression, dissociated commissural neurons treated with the E3 ligase inhibitor Heclin exhibit a significantly stronger response to Slit in growth cone collapse assays. These observations, combined with our biochemical and genetic data strongly support an important role for Nedd4-directed Robo1 regulation in allowing commissural axons to cross the midline.

Our *in vitro* and *in vivo* evidence reveal striking similarities between the function of Ndfip proteins and the function of *Drosophila* Comm; however, in contrast to the complete absence of midline crossing in *comm* mutants, even complete removal of Ndfip proteins results in only a partial loss of midline crossing in the developing spinal cord. Perhaps this is not too surprising given the constellation of mechanisms that promote midline crossing in the vertebrate spinal cord that do not appear to be present in *Drosophila*, including additional attractive pathways mediated through Shh and VegF signaling (Gorla and Bashaw, 2020). Most notably is the important role of Robo3, which acts via several mechanisms to promote crossing, including potentiating Dcc signaling, responding to the repulsive Nell2 ligand present in the motor column and indirectly attenuating Robo1 repulsion

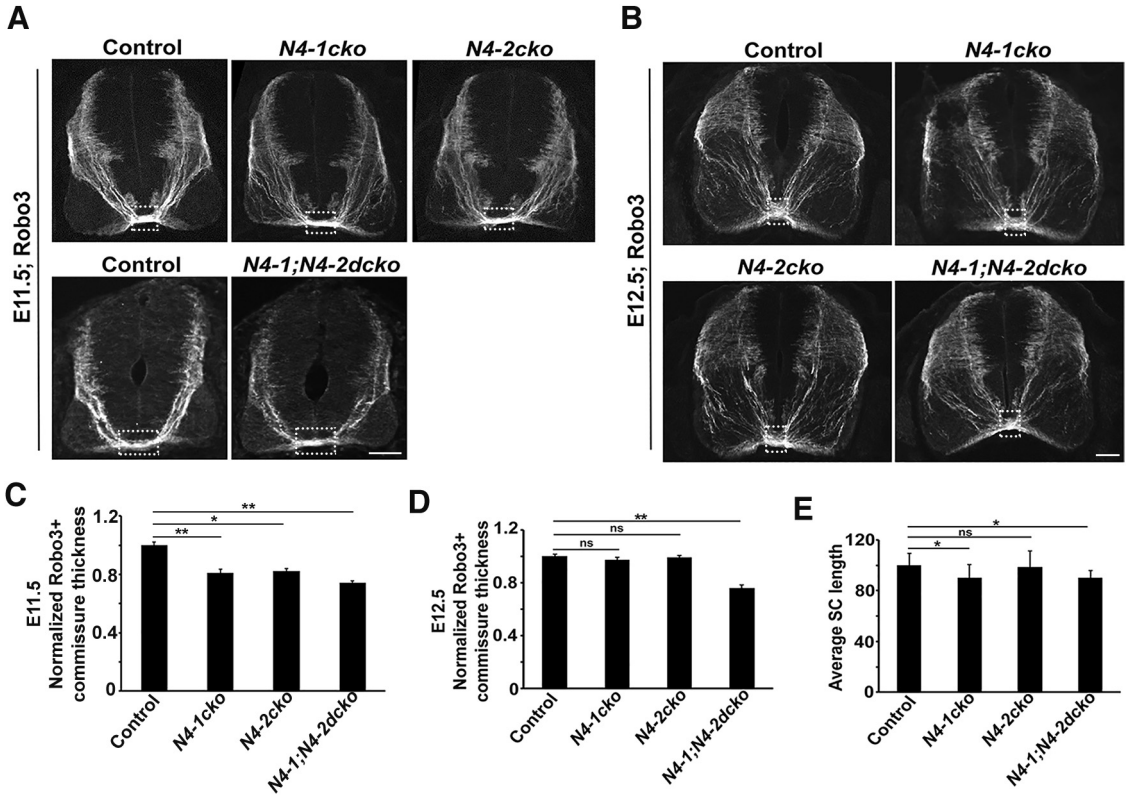

Figure 9. *Nedd4-1* and *Nedd4-2* conditional mutant embryos have commissural axon guidance defects. ***A***, ***B***, Representative confocal images of E11.5 (***A***) and E12.5 (***B***) transverse spinal cord sections that were taken from *Nedd4-1* or *Nedd4-2* or *Nedd4-1; Nedd4-2* conditional mutant embryos and from sibling control mouse embryos. All sections were immunostained with a Robo3 antibody to label the commissural axon population. In E11.5 *Nedd4-1* and *Nedd4-2* conditional mutant embryos, the Robo3-positive ventral commissure is reduced in thickness relative to sibling controls. The commissure thickness was further decreased in *Nedd4-1; Nedd4-2* conditional double mutant spinal cord sections (***A***). At E12.5, *Nedd4-1; Nedd4-2* double conditional mutant embryos have significantly reduced commissure thickness compared with control or single conditional mutant embryos (***B***). ***C***, ***D***, Quantification of Robo3-positive commissure thickness normalized to the dorsal-ventral length of the spinal cords at E11.5 and E12.5. Data were further normalized to sibling controls. ***E***, Quantification of dorsal-ventral spinal cord length (SC length) of E11.5 control, *Nedd4-1*, *Nedd4-2*, and *Nedd4-1; Nedd4-2* conditional mutant embryos. The quantifications show the mean and SEM of five to eight sections per embryo, where $n = 7$ embryos for control, $n = 3$ embryos for *Nedd4-1* conditional mutants, $n = 3$ embryos for *Nedd4-2* conditional mutants and $n = 2$ embryos for *Nedd4-1; Nedd4-2* double conditional mutants at E11.5. At E12.5, $n = 2$ embryos for control, *Nedd4-1*, *Nedd4-2*, and *Nedd4-1; Nedd4-2* conditional mutants (*n* denotes the number of embryos that were analyzed for each genotype). Significance was assessed by one-way ANOVA. $^{**}p < 0.01$ and $^{*}p < 0.05$. Scale bars: 100 μm. White dashed rectangle in ***A*** and ***B*** shows ventral commissure.

(Sabatier et al., 2004; Zelina et al., 2014; Jaworski et al., 2015). In addition, Robo3, Dcc and Robo1 are all regulated by alternative splicing, and this contributes to the potentiation of Dcc and Robo3-directed midline crossing, as well as in the inhibition of Robo1 responses (Chen et al., 2008; Leggere et al., 2016; Johnson et al., 2019).

Insights into the mechanisms of Nedd4 substrate specificity

Our biochemical analyses show that Ndfip adaptor proteins can interact with all seven of the Nedd4 E3 ligases tested. However, despite the promiscuity of these interactions, only three of the ligases, Nedd4-1, Nedd4-2, and WWP1, can promote the ubiquitylation and degradation of Robo1 *in vitro*. Our data also show that in addition to Nedd4-1 and Nedd4-2, Smurf can also form a ternary complex with Ndfip proteins and Robo1. Together, these results indicate that the interaction with Ndfip adaptors and the subsequent substrate recruitment alone is not sufficient for Nedd4 E3 ligases to target substrates for ubiquitylation, suggesting that there are likely other structural properties or motifs that confer substrate specificity to the different E3 ligases. Interestingly, the substrate recognition sequences for Smurfs differ from those of other Nedd4 ligases (Li et al., 2021), and unlike other Nedd4 family E3 ligases, Smurfs are still able to associate with Ndfip proteins in the absence of their PY motifs (Fig. 1). Alternatively, Smurfs may be unable to mediate Robo1 ubiquitylation because the substrate specificity of Nedd4 E3 ligases appears to be cell type-dependent. For instance, Ndfip-mediated ubiquitylation of the divalent metal ion transporter (DMT1) is mediated by WWP2 in non-neuronal cells (Foot et al., 2008), whereas in human neuronal cells, Nedd4-2 is recruited by Ndfip1 to ubiquitylate DMT1 (Howitt et al., 2009).

Conserved roles for Nedd4 E3 ligases and their adaptors in axon guidance

It has been proposed that Comm's ability to regulate Robo1 and promote midline crossing in *Drosophila* depends on its interaction with the E3 ubiquitin ligase Nedd4 (Myat et al., 2002). This was based on the observations that Comm can physically interact with and be ubiquitylated by Nedd4 *in vitro*, and that mutations in the LPSY and CCPY motifs in the cytoplasmic domain of Comm disrupt its ability to bind to Nedd4, and in turn to regulate Robo1 (Myat et al., 2002). This model was directly challenged by a subsequent report (Keleman et al., 2005). Specifically, it was shown that a mutant version of Comm that cannot be ubiquitylated can fully restore Comm's activity and that embryos homozygous for a chromosomal deletion of *Nedd4* have no obvious commissural guidance defects (Keleman et al., 2005).

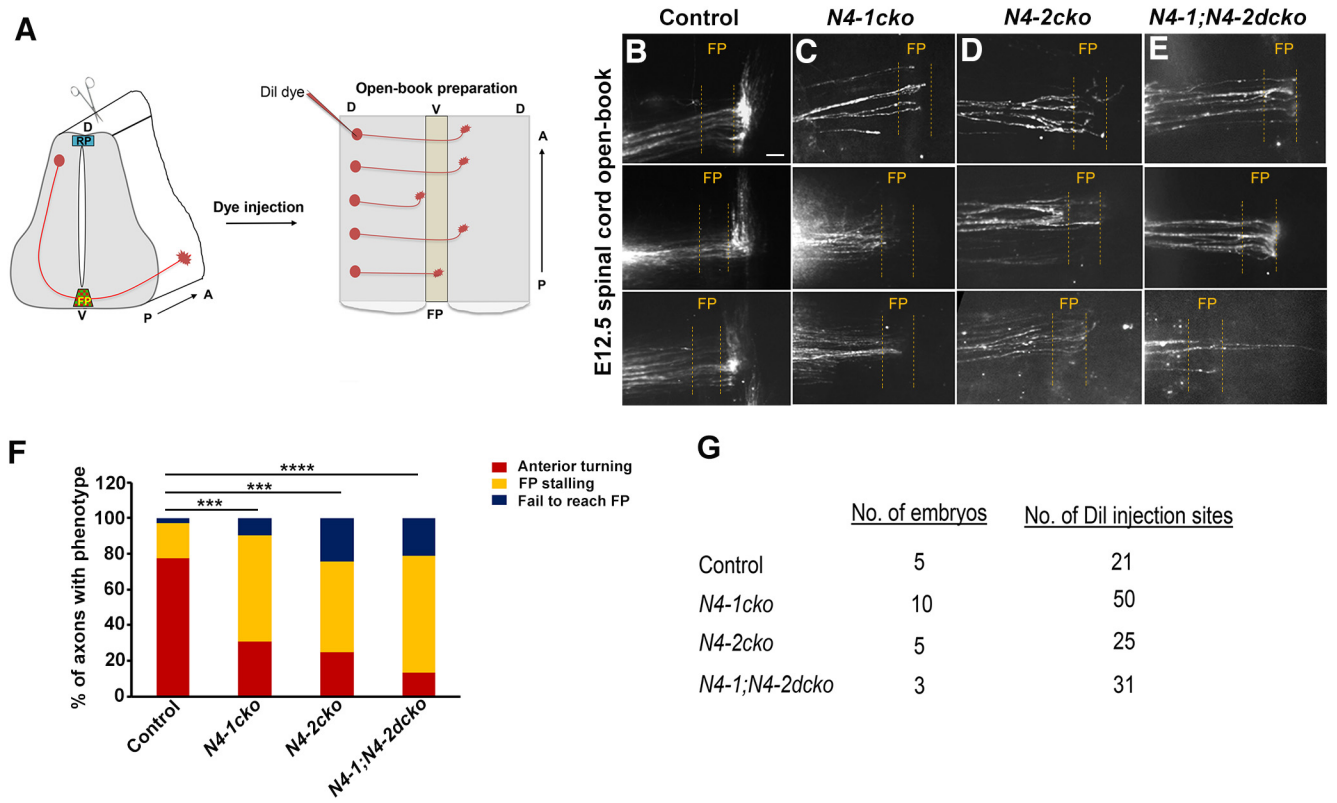

G

	No. of embryos	No. of Dil injection sites
Control	5	21
N4-1cko	10	50
N4-2cko	5	25
N4-1;N4-2dcko	3	31

Figure 10. Commissural axons in Nedd4 conditional mutants fail to enter the floor plate normally. ***A***, Schematic of spinal cord open-book preparation and Dil injection into dorsal spinal commissural neuron cell bodies. Spinal cords were isolated from E12.5 mouse embryos and open-books were prepared by making a cut at the roof plate. Using a fine needle, Dil dye was injected into the cell bodies of commissural axons that are located on the dorsal side. ***B–E***, Confocal images of Dil injections in E12.5 spinal cord open-book preparations marking commissural axons. Three representative images are shown for each indicated genotype. In control open-book spinal cord preparations, the majority of axons crossed the floor plate and turned anteriorly on the contralateral side (***B***). In *Nedd4-1* and *Nedd4-2* conditional single mutant open-book preparations, labeled commissural axons frequently stall in the floor plate and fail to exit and make the correct anterior turn. In a few embryos, some axons fail to even reach the floor plate (***C***, ***D***). In *Nedd4-1; Nedd4-2* conditional double mutant open-books, these phenotypes are significantly stronger than those observed in the single conditional mutant cords (***E***). ***F***, The bar graph represents the percentage of axons with the indicated phenotypes. The percentage of axons that turned anteriorly is significantly decreased in *Nedd4-1*, *Nedd4-2*, and *Nedd4-1; Nedd4-2* conditional mouse embryos compared with sibling controls. ***G***, The table represents the number of embryos and the number of Dil injection sites that were analyzed and quantified in ***F***. Control; $n = 5$ with number of injection sites 21, *Nedd4-1* conditional single mutant; $n = 10$ with number of injection sites 50, *Nedd4-2* conditional single mutant; $n = 5$ with number of injection sites 25 and *Nedd4-1; Nedd4-2* conditional double mutant; $n = 3$ with number of injection sites 31 (n = number of embryos analyzed for each genotype). Significance for anterior turning phenotype was assessed by one-way ANOVA, $^{**}p < 0.0001$ and $^{***}p < 0.00001$. Scale bars: 50 µm. FP, floor plate; A, anterior; P, posterior; D, dorsal; V, ventral.

While these observations would appear to preclude an important role for the ubiquitylation of Comm for its ability to negatively regulate Robo1, they do not definitively rule out a role for Nedd4 E3 ligases in commissural axon guidance. First, whether the Robo1 receptor could be a Nedd4 substrate was never explored. Additionally, Nedd4 mRNA is maternally deposited, potentially masking the effects of removing Nedd4 zygotically. Furthermore, there are two other Nedd4 family members in *Drosophila*: Suppressor of deltex [Su(dx)] and dSmurf (Dalton et al., 2011). Given these considerations and our study, whether E3 ubiquitin ligase activity is required in *Drosophila* for the regulation of Robo1 is still an open question.

How is the activity of Nedd4 regulated?

One potential mechanism to control the activity of the Nedd4 ligases would be to regulate the binding of Ndfip proteins to Nedd4. In principle, this could be achieved by controlling the expression, localization or binding properties of Ndfip proteins. Interestingly, our previous observations that Ndfip1 is enriched in commissural axons as they are crossing the midline positions it to transiently inhibit Robo1 expression (Gorla et al., 2019). Indeed, Ndfip protein localization is reminiscent of the enrichment of Comm in precrossing commissural axons in *Drosophila*. The expression of *comm* mRNA is under tight spatial and temporal control, peaking as commissural axons extend into the midline before being turned off on midline exit (Keleman et al., 2002). Comm transcription is regulated, in part by Fra, the *Drosophila* ortholog of Dcc. The transcriptional activity of Fra depends on γ-secretase proteolysis, which releases the intracellular domain of Fra, allowing it to enter the nucleus where it activates *comm* transcription (Yang et al., 2009; Neuhaus-Follini and Bashaw, 2015a). Dcc is also cleaved by γ-secretase, and its ICD can enter the nucleus to regulate gene expression *in vitro* (Taniguchi et al., 2003; Bai et al., 2011). Thus, it will be interesting to determine whether Dcc regulates the transcription of Ndfip1 and Ndfip2. Ndfip proteins are also known to be regulated post-translationally through ubiquitylation by Nedd4 family proteins (Harvey et al., 2002; Shearwin-Whyatt et al., 2004). Interestingly, we have found that preventing the association of Ndfip1 with Nedd4 has a profound stabilizing effect on the Ndfip1 protein (Gorla et al., 2019). The possibility that Ndfip1 could be ubiquitylated and degraded together with its substrate would also be consistent with the transient downregulation of Robo1.

Ndfip, Nedd4, and the regulation of other axon guidance molecules

While our data indicate that Nedd4 proteins regulate Robo1 ubiquitylation and degradation, our results do not exclude the possibility that Nedd4 proteins regulate other substrates to promote midline crossing. Indeed, a previous study in *Drosophila* provides strong evidence that Comm must regulate substrates in addition to Robo1 to allow commissural axons to cross the midline (Gilestro, 2008). In this study, the endogenous Robo1 gene was replaced with a variant of Robo1 that cannot be regulated by Comm. If Robo1 were the only substrate for Comm, then this manipulation should result in premature Robo1 repulsion and a failure of all axons to cross the midline, as in *comm* mutants. Strikingly, embryos bearing this unregulated Robo1 receptor show no deficits in midline crossing (Gilestro, 2008), indicating that other important substrates remain to be identified. It will be interesting in future studies to determine whether Comm and Ndfip proteins share additional substrates that are important for midline crossing. Identification of additional substrates of the Ndfip-Nedd4 trafficking pathway will offer new insights into axon guidance in the developing spinal cord, and will also inform studies of this pathway in other tissue contexts.

References

Bai G, Chivatakarn O, Bonanomi D, Lettieri K, Franco L, Xia C, Stein E, Ma L, Lewcock JW, Pfaff SL (2011) Presenilin-dependent receptor processing is required for axon guidance. Cell 144:106–118.

Blockus H, Chédotal A (2016) Slit-Robo signaling. Development 143:3037–3044.

Brose K, Bland KS, Wang KH, Arnott D, Henzel W, Goodman CS, Tessier-Lavigne M, Kidd T (1999) Slit proteins bind Robo receptors and have an evolutionarily conserved role in repulsive axon guidance. Cell 96:795–806.

Charron F, Stein E, Jeong J, McMahon AP, Tessier-Lavigne M (2003) The morphogen sonic hedgehog is an axonal chemoattractant that collaborates with netrin-1 in midline axon guidance. Cell 113:11–23.

Chaudhari K, Gorla M, Chang C, Kania A, Bashaw GJ (2021) Robo recruitment of the Wave regulatory complex plays an essential and conserved role in midline repulsion. Elife 10:e64474.

Chen Z, Gore BB, Long H, Ma L, Tessier-Lavigne M (2008) Alternative splicing of the Robo3 axon guidance receptor governs the midline switch from attraction to repulsion. Neuron 58:325–332.

Dalton HE, Denton D, Foot NJ, Ho K, Mills K, Brou C, Kumar S (2011) *Drosophila* Ndfip is a novel regulator of Notch signaling. Cell death Differ 18:1150–1160.

Dickson BJ, Zou Y (2010) Navigating intermediate targets: the nervous system midline. Cold Spring Harb Perspect Biol 2:a002055.

Evans TA, Bashaw GJ (2012) Slit/Robo-mediated axon guidance in *Tribolium* and *Drosophila*: divergent genetic programs build insect nervous systems. Dev Biol 363:266–278.

Evans TA, Santiago C, Arbeille E, Bashaw GJ (2015) Robo2 acts in trans to inhibit Slit-Robo1 repulsion in pre-crossing commissural axons. Elife 4:e08407.

Foot NJ, Dalton HE, Shearwin-Whyatt LM, Dorstyn L, Tan SS, Yang B, Kumar S (2008) Regulation of the divalent metal ion transporter DMT1 and iron homeostasis by a ubiquitin-dependent mechanism involving Ndfips and WWP2. Blood 112:4268–4275.

Gilestro GF (2008) Redundant mechanisms for regulation of midline crossing in *Drosophila*. PLoS One 3:e3798.

Gorla M, Bashaw GJ (2020) Molecular mechanisms regulating axon responsiveness at the midline. Dev Biol 466:12–21.

Gorla M, Santiago C, Chaudhari K, Layman AAK, Oliver PM, Bashaw GJ (2019) Ndfip proteins target Robo receptors for degradation and allow commissural axons to cross the midline in the developing spinal cord. Cell Rep 26:3298–3312.e4.

Harvey KF, Shearwin-Whyatt LM, Fotia A, Parton RG, Kumar S (2002) N4WBP5, a potential target for ubiquitination by the Nedd4 family of proteins, is a novel Golgi-associated protein. J Biol Chem 277:9307–9317.

Howitt J, Putz U, Lackovic J, Doan A, Dorstyn L, Cheng H, Yang B, Chan-Ling T, Silke J, Kumar S, Tan SS (2009) Divalent metal transporter 1 (DMT1) regulation by Ndfip1 prevents metal toxicity in human neurons. Proc Natl Acad Sci U S A 106:15489–15494.

Hsia HE, Kumar R, Luca R, Takeda M, Courchet J, Nakashima J, Wu S, Goebbels S, An W, Eickholt BJ, Polleux F, Rotin D, Wu H, Rossner MJ, Bagni C, Rhee JS, Brose N, Kawabe H (2014) Ubiquitin E3 ligase Nedd4-1 acts as a downstream target of PI3K/PTEN-mTORC1 signaling to promote neurite growth. Proc Natl Acad Sci U S A 111:13205–13210.

Ishii N, Wadsworth WG, Stern BD, Culotti JG, Hedgecock EM (1992) UNC-6, a laminin-related protein, guides cell and pioneer axon migrations in *C. elegans*. Neuron 9:873–881.

Jaworski A, Tom I, Tong RK, Gildea HK, Koch AW, Gonzalez LC, Tessier-Lavigne M (2015) Operational redundancy in axon guidance through the multifunctional receptor Robo3 and its ligand NELL2. Science 350:961–965.

Johnson V, Junge HJ, Chen Z (2019) Temporal regulation of axonal repulsion by alternative splicing of a conserved microexon in mammalian Robo1 and Robo2. Elife 8:e46042.

Kawabe H, Neeb A, Dimova K, Young SM Jr, Takeda M, Katsurabayashi S, Mitkovski M, Malakhova OA, Zhang DE, Umikawa M, Kariya K, Goebbels S, Nave KA, Rosenmund C, Jahn O, Rhee J, Brose N (2010) Regulation of Rap2A by the ubiquitin ligase Nedd4-1 controls neurite development. Neuron 65:358–372.

Keleman K, Rajagopalan S, Cleppien D, Teis D, Paiha K, Huber LA, Technau GM, Dickson BJ (2002) Comm sorts robo to control axon guidance at the *Drosophila* midline. Cell 110:415–427.

Keleman K, Ribeiro C, Dickson BJ (2005) Comm function in commissural axon guidance: cell-autonomous sorting of Robo in vivo. Nat Neurosci 8:156–163.

Kidd T, Russell C, Goodman CS, Tear G (1998) Dosage-sensitive and complementary functions of roundabout and commissureless control axon crossing of the CNS midline. Neuron 20:25–33.

Kidd T, Bland KS, Goodman CS (1999) Slit is the midline repellent for the robo receptor in *Drosophila*. Cell 96:785–794.

Kimura T, Kawabe H, Jiang C, Zhang W, Xiang YY, Lu C, Salter MW, Brose N, Lu WY, Rotin D (2011) Deletion of the ubiquitin ligase Nedd4L in lung epithelia causes cystic fibrosis-like disease. Proc Natl Acad Sci U S A 108:3216–3221.

Kinoshita-Kawada M, Hasegawa H, Hongu T, Yanagi S, Kanaho Y, Masai I, Mishima T, Chen X, Tsuboi Y, Rao Y, Yuasa-Kawada J, Wu JY (2019) A crucial role for Arf6 in the response of commissural axons to Slit. Development 146:dev172106.

Leggere JC, Saito Y, Darnell RB, Tessier-Lavigne M, Junge HJ, Chen Z (2016) NOVA regulates Dcc alternative splicing during neuronal migration and axon guidance in the spinal cord. Elife 5:e14264.

Li Z, Chen S, Jhong JH, Pang Y, Huang KY, Li S, Lee TY (2021) UbiNet 2.0: a verified, classified, annotated and updated database of E3 ubiquitin ligase-substrate interactions. Database (Oxford) 2021:baab010.

Lyuksyutova AI, Lu CC, Milanesio N, King LA, Guo N, Wang Y, Nathans J, Tessier-Lavigne M, Zou Y (2003) Anterior-posterior guidance of commissural axons by Wnt-frizzled signaling. Science 302:1984–1988.

Mitchell KJ, Doyle JL, Serafini T, Kennedy TE, Tessier-Lavigne M, Goodman CS, Dickson BJ (1996) Genetic analysis of Netrin genes in *Drosophila*: netrins guide CNS commissural axons and peripheral motor axons. Neuron 17:203–215.

Mund T, Pelham HR (2009) Control of the activity of WW-HECT domain E3 ubiquitin ligases by NDFIP proteins. EMBO Rep 10:501–507.

Mund T, Pelham HR (2010) Regulation of PTEN/Akt and MAP kinase signaling pathways by the ubiquitin ligase activators Ndfip1 and Ndfip2. Proc Natl Acad Sci U S A 107:11429–11434.

Mund T, Lewis MJ, Maslen S, Pelham HR (2014) Peptide and small molecule inhibitors of HECT-type ubiquitin ligases. Proc Natl Acad Sci U S A 111:16736–16741.

Myat A, Henry P, McCabe V, Flintoft L, Rotin D, Tear G (2002) *Drosophila* Nedd4, a ubiquitin ligase, is recruited by Commissureless to control cell surface levels of the roundabout receptor. Neuron 35:447–459.

Neuhaus-Follini A, Bashaw GJ (2015a) The intracellular domain of the frazzled/DCC receptor is a transcription factor required for commissural axon guidance. Neuron 87:751–763.

Neuhaus-Follini AB, Bashaw GJ (2015b) Crossing the embryonic midline: molecular mechanisms regulating axon responsiveness at an intermediate target. Wiley Interdiscip Rev Dev Biol 4:377–389.

Sabatier C, Plump AS, Le M, Brose K, Tamada A, Murakami F, Lee EY, Tessier-Lavigne M (2004) The divergent Robo family protein rig-1/Robo3 is a negative regulator of slit responsiveness required for midline crossing by commissural axons. Cell 117:157–169.

Serafini T, Colamarino SA, Leonardo ED, Wang H, Beddington R, Skarnes WC, Tessier-Lavigne M (1996) Netrin-1 is required for commissural axon guidance in the developing vertebrate nervous system. Cell 87:1001–1014.

Shearwin-Whyatt LM, Brown DL, Wylie FG, Stow JL, Kumar S (2004) N4WBP5A (Ndfip2), a Nedd4-interacting protein, localizes to multivesicular bodies and the Golgi, and has a potential role in protein trafficking. J Cell Sci 117:3679–3689.

Taniguchi Y, Kim SH, Sisodia SS (2003) Presenilin-dependent "gamma-secretase" processing of deleted in colorectal cancer (DCC). J Biol Chem 278:30425–30428.

Trimpert C, Wesche D, de Groot T, Pimentel Rodriguez MM, Wong V, van den Berg DTM, Cheval L, Ariza CA, Doucet A, Stagljar I, Deen PMT (2017) NDFIP allows NEDD4/NEDD4L-induced AQP2 ubiquitination and degradation. PLoS One 12:e0183774.

Vallstedt A, Kullander K (2013) Dorsally derived spinal interneurons in locomotor circuits. Ann N Y Acad Sci 1279:32–42.

Yang L, Garbe DS, Bashaw GJ (2009) A frazzled/DCC-dependent transcriptional switch regulates midline axon guidance. Science 324:944–947.

Zelina P, Blockus H, Zagar Y, Péres A, Friocourt F, Wu Z, Rama N, Fouquet C, Hohenester E, Tessier-Lavigne M, Schweitzer J, Roest Crollius H, Chédotal A (2014) Signaling switch of the axon guidance receptor Robo3 during vertebrate evolution. Neuron 84:1258–1272.

Zou Y, Stoeckli E, Chen H, Tessier-Lavigne M (2000) Squeezing axons out of the gray matter: a role for slit and semaphorin proteins from midline and ventral spinal cord. Cell 102:363–375.